

Connecting Satellite Observations with Water Cycle Variables Through Land Data Assimilation: Examples Using the NASA GEOS-5 LDAS

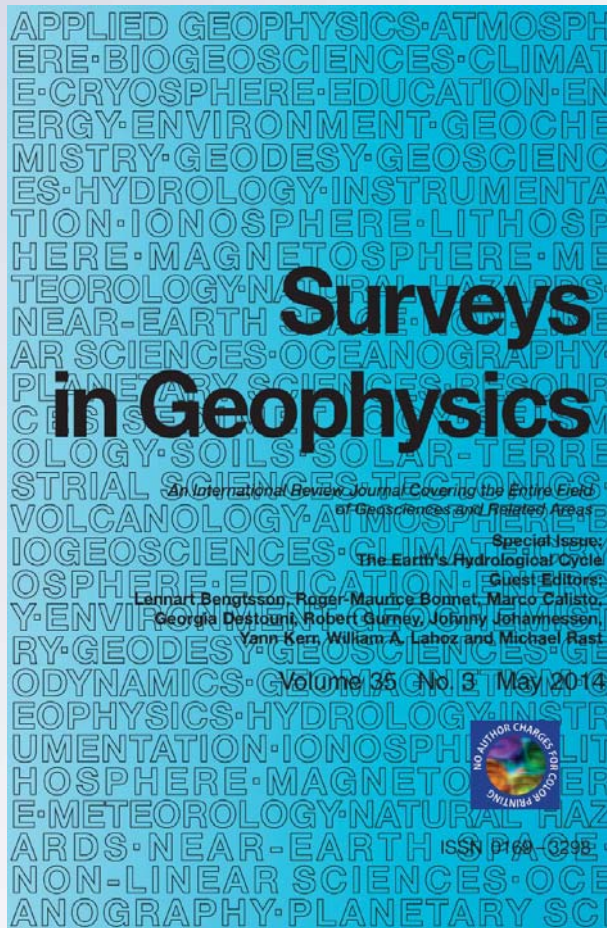
Rolf H. Reichle, Gabriëlle J. M. De Lannoy, Barton A. Forman, Clara S. Draper & Qing Liu

Surveys in Geophysics

An International Review Journal
Covering the Entire Field of Geosciences
and Related Areas

ISSN 0169-3298
Volume 35
Number 3

Surv Geophys (2014) 35:577-606
DOI 10.1007/s10712-013-9220-8



Your article is protected by copyright and all rights are held exclusively by Springer Science+Business Media Dordrecht (outside the USA). This e-offprint is for personal use only and shall not be self-archived in electronic repositories. If you wish to self-archive your article, please use the accepted manuscript version for posting on your own website. You may further deposit the accepted manuscript version in any repository, provided it is only made publicly available 12 months after official publication or later and provided acknowledgement is given to the original source of publication and a link is inserted to the published article on Springer's website. The link must be accompanied by the following text: "The final publication is available at link.springer.com".

Connecting Satellite Observations with Water Cycle Variables Through Land Data Assimilation: Examples Using the NASA GEOS-5 LDAS

Rolf H. Reichle · Gabriëlle J. M. De Lannoy · Barton A. Forman · Clara S. Draper · Qing Liu

Received: 7 September 2012 / Accepted: 22 January 2013 / Published online: 15 February 2013
© Springer Science+Business Media Dordrecht (outside the USA) 2013

Abstract A land data assimilation system (LDAS) can merge satellite observations (or retrievals) of land surface hydrological conditions, including soil moisture, snow, and terrestrial water storage (TWS), into a numerical model of land surface processes. In theory, the output from such a system is superior to estimates based on the observations or the model alone, thereby enhancing our ability to understand, monitor, and predict key elements of the terrestrial water cycle. In practice, however, satellite observations do not correspond directly to the water cycle variables of interest. The present paper addresses various aspects of this seeming mismatch using examples drawn from recent research with the ensemble-based NASA GEOS-5 LDAS. These aspects include (1) the assimilation of coarse-scale observations into higher-resolution land surface models, (2) the partitioning of satellite observations (such as TWS retrievals) into their constituent water cycle components, (3) the forward modeling of microwave brightness temperatures over land for radiance-based soil moisture and snow assimilation, and (4) the selection of the most relevant types of observations for the analysis of a specific water cycle variable that is not observed (such as root zone soil moisture). The solution to these challenges involves the careful construction of an observation operator that maps from the land surface model variables of interest to the space of the assimilated observations.

Keywords Land data assimilation · Land surface modeling · Satellite remote sensing · Soil moisture · Snow · Terrestrial water storage · Ensemble Kalman filter

R. H. Reichle (✉) · G. J. M. De Lannoy · C. S. Draper · Q. Liu
Global Modeling and Assimilation Office (Code 610.1), NASA Goddard Space Flight Center,
8800 Greenbelt Road, Greenbelt, MD 20771, USA
e-mail: rolf.reichle@nasa.gov

G. J. M. De Lannoy · C. S. Draper
Universities Space Research Association, Columbia, MD, USA

B. A. Forman
Department of Civil and Environmental Engineering, University of Maryland, College Park, MD, USA

Q. Liu
Science Systems and Applications, Inc., Lanham, MD, USA

1 Introduction

The water cycle plays a crucial role in Earth's climate and environment, yet there are still large gaps in our understanding of its components, particularly at the land surface (Lahoz and De Lannoy 2013; Trenberth and Asrar 2013). Over the past decade, there has been a steady increase in the number and types of satellite observations (or retrievals) related to land surface hydrological conditions, including soil moisture, snow, and terrestrial water storage (TWS; Bartalis et al. 2007; Bruinsma et al. 2010; Clifford 2010; de Jeu et al. 2008; Entekhabi et al. 2010; Foster et al. 2005, 2011; Gao et al. 2010; Hall and Riggs 2007; Hall et al. 2010; Horwath et al. 2011; Kelly 2009; Kerr et al. 2010; Li et al. 2007; Liu et al. 2011b; Njoku et al. 2003; Parinussa et al. 2012; Pulliainen 2006; Rowlands et al. 2005, 2010; Swenson and Wahr 2006; Tedesco and Narvekar 2010; Tedesco et al. 2010; Wahr et al. 2004).

These observations can be assimilated into land surface models to provide land surface hydrological estimates that are generally superior to the satellite observations or model estimates alone (Andreadis and Lettenmaier 2006; Crow and Wood 2003; De Lannoy et al. 2012; de Rosnay et al. 2012a, b; Draper et al. 2012; Drusch 2007; Dunne and Entekhabi 2006; Durand and Margulis 2008; Forman et al. 2012; Houborg et al. 2012; Li et al. 2012; Liu et al. 2011a; Margulis et al. 2002; Pan and Wood 2006; Pan et al. 2008; Reichle and Koster 2005; Reichle et al. 2007, 2009; Sahoo et al. 2012; Su et al. 2008, 2010; Zaitchik et al. 2008).

However, land data assimilation systems must be designed carefully such that a number of conceptual problems can be overcome and the potential improvements from data assimilation can be realized. Earlier work addressed the bias between the satellite observations and model estimates within the assimilation system (De Lannoy et al. 2007; Drusch et al. 2005; Kumar et al. 2012; Reichle and Koster 2004). Moreover, approaches to efficient error modeling within the assimilation system, including adaptive methods, needed to be developed (Crow and Reichle 2008; Crow and van den Berg 2010; Reichle et al. 2008a, b). An overview of some relevant earlier literature in the context of the ensemble-based Goddard Earth Observing System Model, Version 5 (GEOS-5) land data assimilation system (LDAS) developed at the NASA Global Modeling and Assimilation Office (GMAO) is provided by Reichle et al. (2009).

Despite the early successes, the design and application of land data assimilation systems still face additional conceptual problems. While land surface models are flexible in the design and choice of model variables, satellite observations do not necessarily correspond directly to the water cycle variables of interest. For example, space-borne microwave observations can be converted into estimates of snow amount or surface soil moisture, but the spatial resolution of such microwave-based retrievals is usually much coarser than desired. Moreover, satellites typically observe electromagnetic properties such as backscatter and/or radiances (or brightness temperatures) that are only indirectly related to snow amounts or soil moisture levels. Furthermore, satellite-observed backscatter and radiances are at best sensitive to moisture in the top few centimeters of the soil. Information on important water cycle components such as root zone soil moisture must therefore be gained through even more indirect pathways in the land data assimilation system.

The present paper addresses several major challenges that all relate to a seeming mismatch between the assimilated observations and the water cycle variables of interest. This mismatch can be overcome through the careful design of the land data assimilation system. The conceptual challenges discussed here can be summarized as follows:

1. How can coarse-scale satellite observations increase our knowledge of land surface conditions at finer scales (horizontal downscaling), and how can unobserved areas be updated using information from neighboring observations?
2. How can vertically integrated measurements (such as TWS) be partitioned into their component variables within the assimilation system?
3. How can satellite radiances (rather than geophysical retrievals) be assimilated to improve estimates of land surface hydrological conditions (e.g., soil moisture and snow)?
4. How can the most relevant types of observations be selected for the analysis of a water cycle component that is not observed (such as root zone soil moisture)?

The present paper illustrates each of these conceptual problems based on recent progress using the GEOS-5 system for land surface hydrological data assimilation. The examples use satellite observations of land surface water cycle components from the Advanced Microwave Scanning Radiometer for EOS (AMSR-E), the Moderate Resolution Imaging Spectroradiometer (MODIS), the Gravity Recovery and Climate Experiment (GRACE) mission, the Advanced Scatterometer (ASCAT), and the Soil Moisture Ocean Salinity (SMOS) mission for the analysis of soil moisture (AMSR-E, ASCAT, SMOS, GRACE), snow (AMSR-E, MODIS, GRACE), and TWS (GRACE). After a brief discussion of the GEOS-5 LDAS, Sect. 2 provides details and references for the various satellite observations used in the examples. Section 3 addresses each of the above-mentioned challenge questions in a separate subsection. Results are discussed and summarized in Sect. 4. Finally, Sect. 5 provides conclusions and a brief outlook on future research directions.

2 Data and Methods

2.1 GEOS-5 Land Data Assimilation System

The GEOS-5 LDAS consists of the NASA Catchment land surface model and an implementation of the ensemble Kalman filter (EnKF; Evensen 2003). The GEOS-5 EnKF has also been included in the NASA Land Information System, a comprehensive land surface modeling and assimilation software framework, so that it can be used with a variety of land surface models (Kumar et al. 2008a, b). A brief summary of the key characteristics of the system is provided below. For a more comprehensive discussion, see Reichle et al. (2009) and references therein.

The Catchment land surface model (hereinafter Catchment model; Ducharme et al. 2000; Koster et al. 2000) differs from traditional, layer-based land surface models by including an explicit treatment of the spatial variation within each hydrological catchment (or computational element) of the soil water and water table depth, as well as its effect on runoff and evaporation. Within each element, the vertical profile of soil water down to the bedrock is given by the equilibrium soil moisture profile and the deviations from the equilibrium profile. The deviations are described by excess and deficit variables for a 0–2 cm (or 0–5 cm) surface layer and for a “root zone” layer that extends from the surface to a depth z_R of $75 \text{ cm} \leq z_R \leq 100 \text{ cm}$ depending on local soil conditions. The spatial variability of soil moisture is diagnosed at each time step from the bulk water prognostic variables and the statistics of the catchment topography. One key feature of the Catchment model is the groundwater component implicit in the modeling of the water table depth (through the modeling of the subsurface water profile down to the bedrock). This

groundwater component is critically important for the assimilation of TWS retrievals (Sect. 3.2).

The Catchment model also includes a state-of-the-art, multi-layer, global snow model (Stieglitz et al. 2001). In each watershed, the evolution of the amount of water in the snow pack (or snow water equivalent; SWE), the snow depth, and the snow heat content in response to surface meteorological conditions and snow compaction is modeled using three layers. The soil, vegetation, and snow model parameters used in the Catchment model are from the NASA GEOS-5 global modeling system (Rienecker et al. 2008).

The EnKF is a Monte-Carlo variant of the Kalman filter, which sequentially updates model forecasts in response to observations based on the relative uncertainty of the model and the observations. The key idea behind the EnKF is that the relevant parts of the model error covariance structure can be captured by a small ensemble of model trajectories. Each member of the ensemble experiences perturbed instances of the observed forcing fields (representing errors in the forcing data) and/or randomly generated noise that is added to the model parameters and prognostic variables (representing errors in model physics and parameters). The model error covariance matrices that are required for the filter update can then be diagnosed from the ensemble at the update time. The EnKF is flexible in its treatment of errors in model dynamics and parameters. It is also very suitable for modestly nonlinear problems and has become a popular choice for land data assimilation (Andreadis and Lettenmaier 2006; Durand and Margulis 2008; Kumar et al. 2008a, b; Pan and Wood 2006; Reichle et al. 2002a, b; Su et al. 2008; Zhou et al. 2006).

To realize the potential benefits from data assimilation, the assimilation system must be supplied with appropriate input parameters for the description of model and observation errors. For an ensemble-based system such as the GEOS-5 LDAS, for example, standard deviations, spatial and temporal correlations, and cross-correlations must be specified for the perturbations that are applied to each ensemble member. A detailed discussion of the error parameters in the examples discussed here is beyond the scope of the paper. The reader is referred to the references provided with each example as well as the overview discussion of Reichle et al. (2009).

2.2 Assimilated Observations

The data assimilation examples discussed in this paper use various types of satellite observations from a number of polar orbiting sensors/platforms, including passive and active microwave observations (AMSR-E, SMOS, and ASCAT), visible and near-infrared observations (MODIS), and gravimetric observations (GRACE).

AMSR-E, which operated with nominal performance between 2002 and 2011, is a scanning, dual polarization radiometer that measured microwave emission from the Earth at six frequencies (6.9, 10.7, 18.7, 23.9, 36.5, and 89.0 GHz), ranging in resolution from ~50 km at 6.9 GHz to ~5 km at 89.0 GHz (Knowles et al. 2006). Its successor, AMSR2, was launched in May 2012 (http://www.jaxa.jp/projects/sat/gcom_w/index_e.html). The training and validation of the empirical microwave radiative transfer model for snow-covered land surfaces in Sect. 3.3.2 uses the 10.7, 18.7, and 36.5 GHz AMSR-E brightness temperatures, while the snow assimilation example in Sect. 3.1 uses SWE retrievals that are based on the difference between the 18.7 and the 36.5 GHz brightness temperatures (Kelly 2009). The soil moisture assimilation examples in Sect. 3.4 use surface (top 1 cm) soil moisture retrievals that are derived from the 6.9 and 10.7 GHz brightness temperatures (de Jeu et al. 2008; Njoku et al. 2003).

SMOS was launched in 2009 and its Microwave Imaging Radiometer with Aperture Synthesis (MIRAS) sensor provides multi-angular L-band (1.4 GHz) brightness temperature observations at horizontal and vertical polarization and a nominal spatial resolution of 43 km (Kerr et al. 2010). SMOS brightness temperatures are used in Sect. 3.3.1.

ASCAT is a 5.3 GHz radar system that illuminates the Earth's surface and measures the energy scattered back to the instrument. The ASCAT surface (top 1 cm) soil moisture retrievals used in Sect. 3.4.2 are derived from these backscatter measurements (Bartalis et al. 2007; Wagner et al. 1999) and are provided in units of degree of saturation.

MODIS (2000-present) provides visible and near-infrared observations from which snow cover fraction (SCF) can be retrieved under clear-sky conditions (Hall and Riggs 2007). High-resolution (500 m) MODIS SCF retrievals are in Sect. 3.1.

Through the measurement of gravitational anomalies associated with the accumulation (or loss) of mass near the Earth's surface, GRACE provides approximately monthly, basin-scale ($>150,000 \text{ km}^2$) estimates of variations in TWS, which includes snow, ice, surface water, soil moisture, and groundwater (Bruinsma et al. 2010; Horwath et al. 2011; Rodell et al. 2009; Rowlands et al. 2005, 2010; Swenson and Wahr 2006; Tang et al. 2010; Wahr et al. 2004). The assimilation experiments of Sect. 3.2 use GRACE TWS retrievals.

2.3 Validation Data and Approach

For each of the examples presented in Sect. 3, the output from the assimilation system was evaluated against independent data from various sources. In Sect. 3.1, in situ SWE measurements from United States Department of Agriculture Snowpack Telemetry (SNOTEL; Schaefer et al. 2007) network sites in Colorado were used for evaluation, along with snow depth measurements from National Oceanic and Atmospheric Administration Cooperative Observer Program (COOP; <http://www.ncdc.noaa.gov>) sites.

SWE estimates for the Mackenzie River basin, used for evaluation in Sect. 3.2, were derived from the daily snow depth product of the Canadian Meteorological Centre (CMC) daily snow analysis (Brasnett 1999; Brown and Brasnett 2010) at a horizontal resolution of approximately 24 km. The CMC snow analysis is based on optimal interpolation of in situ daily snow depth observations and aviation reports with a first-guess field generated from a snow model driven by output from the CMC weather model. Using the snow class map shown in Sturm et al. (1995), SWE estimates were obtained by multiplying the CMC snow depths with the Sturm et al. (2010) snow densities. Furthermore, runoff estimates for the Mackenzie River basin and its major sub-basins provided by the Global Runoff Data Center (GRDC; <http://www.bafg.de/GRDC>) were used in Sect. 3.2.

The radiative transfer models of Sect. 3.3 were evaluated with AMSR-E and SMOS microwave brightness temperatures using a split sample approach in which one portion of the satellite brightness data was used for calibration or training and another, different portion was used for evaluation.

In situ profile soil moisture observations used for evaluation in Sect. 3.4 are from the United States Department of Agriculture Soil Climate Analysis Network (SCAN)/SNOTEL (Schaefer et al. 2007) network in the contiguous US and from the Murrumbidgee Soil Moisture Monitoring Network (Smith et al. 2012) in Australia. Both sets of measurements were subjected to extensive quality control steps, including automatic detection of problematic observations and a visual inspection of the time series prior to using the data for evaluation.

Metrics used for skill assessment include the bias, root mean square error (RMSE), and time series correlation coefficient (R). When specified, anomalies were computed by removing a seasonally varying climatology from the data before computing the metrics.

3 Results

3.1 Assimilation of Sparse and Coarse-Scale Observations

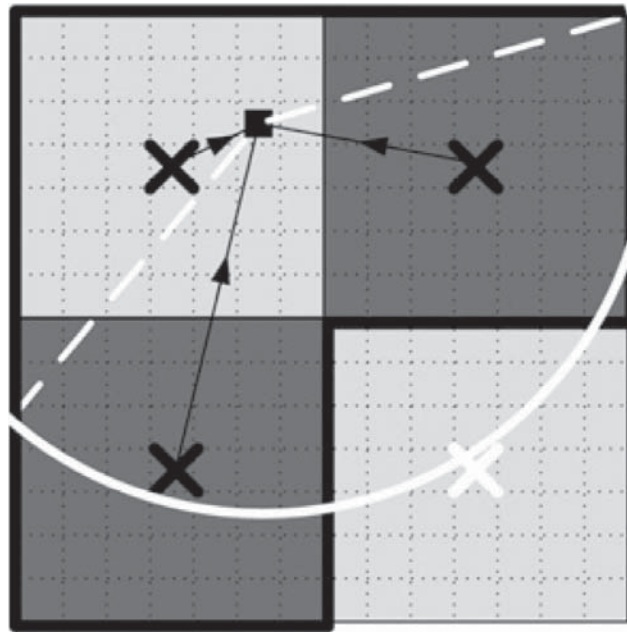
Snow is an important component of the land system because of its strong impact on the land surface water and energy balance, weather, climate, and water resources (Barnett et al. 2005). However, land surface models often represent snow processes poorly. Satellite observations of SWE can be retrieved from passive microwave sensors, but they are only available at relatively coarse resolution. Moreover, SWE retrievals, like most satellite observations, do not provide complete spatial and continuous temporal coverage due to orbit or sensor limitations. The challenge is therefore to design an assimilation system that can use coarse-scale satellite observations to provide enhanced model estimates at the finer scales of interest (horizontal downscaling) and that can also propagate the information to intermittently unobserved areas.

Using AMSR-E SWE retrievals and MODIS SCF observations, De Lannoy et al. (2010, 2012) developed a data assimilation and downscaling technique for estimating fine-scale (1 km) snow fields using coarse-scale (25 km) SWE retrievals and fine-scale (500 m) SCF retrievals for a domain in Northern Colorado, USA. In their study, the authors used the LIS version of the GEOS-5 EnKF together with the Noah land surface model (Ek et al. 2003) (rather than the GEOS-5 LDAS and the Catchment model used elsewhere in this paper). The Noah model simulates a single snow layer with two prognostic variables for SWE and snow depth. The default LIS soil, vegetation, and general parameter tables for Noah were used, including a Noah-specific maximum snow albedo.

Figure 1 shows schematically how the coarse-scale SWE retrievals are used. The fine-scale model grid is represented by the dashed lines in the figure. The coarse-scale grid of the SWE observations is represented by the solid lines and light/dark gray shading, and the center points of individual SWE retrievals are marked with crosses. Let us now consider the analysis update of the fine-scale model grid cell indicated by the solid black square. First, it is important to emphasize that the coarse-scale SWE retrievals are *not* compared directly to the SWE estimate at the fine-scale model grid cell. Rather, the model SWE is aggregated to the coarse grid of the retrievals, that is, the fine-scale model forecast is mapped into the coarse-scale *observation space*. This aggregation is part of the *observation operator* that maps the model states to the observations. Observation-minus-model-forecast residuals (or *innovations*) are then computed at the coarse scale of the observation space. The *Kalman gain* matrix transforms the (observation-space) innovations into the (model-space) *increments*. It is computed from error correlations between the model states at the fine scale and the model-predicted measurements at the coarse scale. Finally, the increments are added to the (fine-scale) model forecast in the *analysis update*. See De Lannoy et al. (2010) for a discussion based on equations.

Second, multiple coarse-scale SWE retrievals in the vicinity of the fine-scale model grid cell in question are used for the analysis update. Specifically, the update uses the three coarse-scale SWE retrievals marked by black crosses that are within a given radius (indicated by the white semi-circle) around the fine-scale model grid cell in question (Fig. 1). Note that this model grid cell would be updated even if the SWE retrieval directly

Fig. 1 Schematic of the distributed (“three-dimensional”) EnKF update used for the assimilation of coarse-scale snow observations. See text for details. Adapted from De Lannoy et al. (2010)



covering it were unavailable—the two neighboring SWE retrievals (dark gray shading) would still contribute to the update. The connection between the neighboring SWE retrievals and the model grid cell in question relies on horizontal model *error* correlations that are due to, for example, errors in large-scale model forcing fields such as snowfall or air temperature.

To assimilate SCF, the Noah model snow depletion curve acts as the observation operator that converts fine-scale modeled SWE into SCF estimates. Unlike binary indicators of snow presence, the continuous SCF observations used here can thus be assimilated with an EnKF, taking advantage of the distribution of SCF values across the ensemble. Snow-free or fully snow-covered conditions in the model-forecast ensemble were addressed by supplementing the EnKF with rule-based update procedures (De Lannoy et al. 2012). If at a given time and location all members of the model-forecast ensemble are snow-free but the SCF observation indicates the presence of snow, then a nominal amount of snow is added to the model forecast. If all forecast ensemble members have full snow cover and the observed SCF indicates less than full cover, then the model-forecast SWE and snow depth are reduced by a fixed fraction.

Figure 2 shows several observed and modeled snow fields for one snow season. The top row shows the coarse-scale (25 km) AMSR-E SWE retrievals, with data missing when the satellite swath does not fully cover the study area. MODIS fine-scale estimates of SCF, shown in the second row, are available only for clear-sky conditions. The bottom four rows of Fig. 2 show that the assimilation of coarse-scale AMSR-E SWE and fine-scale MODIS SCF observations both result in realistic fine-scale spatial SWE patterns.

Through a quantitative validation of the assimilation results with independent measurements at individual SNOTEL and COOP sites over the course of 8 years, De Lannoy et al. (2012) demonstrate improvements from the assimilation of SWE and/or SCF retrievals in shallow snow packs, but not in deep snow packs (not shown). The validation also shows that joint assimilation of SWE and SCF retrievals yields significantly improved RMSE and correlation values. For example, the RMSE for SWE versus COOP site measurements was reduced by 21 % (from 78 to 62 mm) through the joint assimilation of satellite SWE and SCF retrievals. Furthermore, SCF assimilation was found to improve the

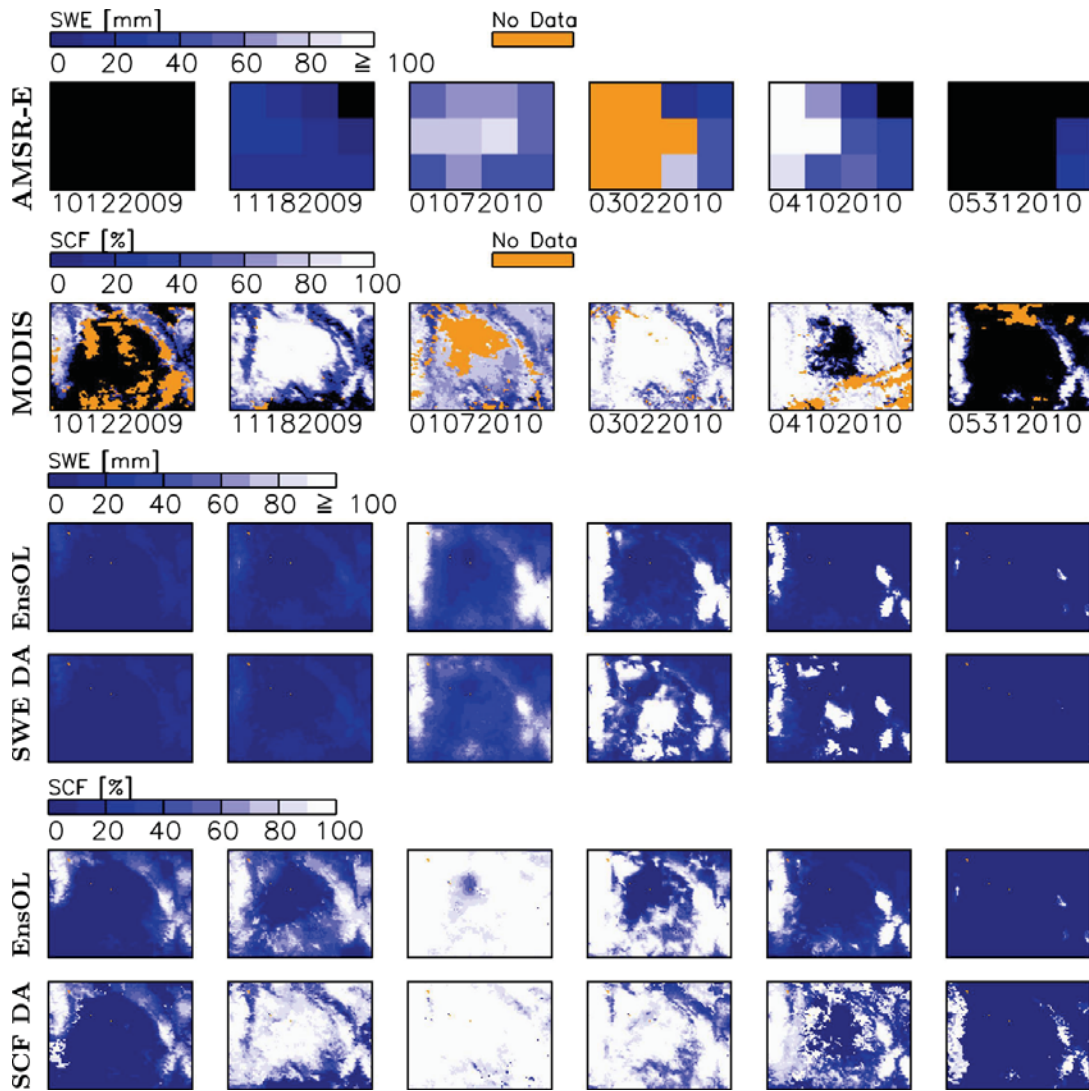


Fig. 2 SWE and SCF fields for 6 days (MMDDYYYY) in the winter of 2009–2010 for a 75 km by 100 km domain (1 km resolution) in northern Colorado. *Blue (white) colors* indicate low (high) SWE or SCF, *black shading* indicates no snow, and *orange shading* indicates no data. The *top two rows* show SWE and SCF satellite observations. The remaining *rows* show SWE (*rows 3 and 4*) and SCF (*rows 5 and 6*) for the ensemble Open Loop (EnsOL) forecast (no assimilation) and the analyses obtained through data assimilation (DA) of SWE or SCF. Adapted from De Lannoy et al. (2012)

timing of the onset of the snow season, albeit without a net improvement of SWE estimates. In areas of deep snow, however, AMSR-E retrievals are typically biased low and require bias correction (or scaling of the observations) prior to data assimilation. De Lannoy et al. (2012) also showed that the interannual SWE variations could not be improved through the assimilation of AMSR-E because the AMSR-E retrievals lack realistic interannual variability in deep snow packs. These deficiencies in the AMSR-E SWE retrievals motivated the development of the empirical microwave radiative transfer model (Sect. 3.3.2) toward a radiance-based snow analysis.

Of course, horizontal downscaling is not only important for snow assimilation. Low-frequency passive microwave brightness temperature observations such those from AMSR-E and SMOS (and the corresponding soil moisture retrievals) are at the coarse resolution of ~ 50 km. But for applications such as weather prediction, soil moisture estimates are

needed at hydrometeorological scales of ~ 10 km or better. Examples of soil moisture downscaling based on data assimilation are provided by Reichle et al. (2001), Sahoo et al. (2012), and Zhou et al. (2006). Also, Reichle and Koster (2003) addressed the propagation of observational soil moisture information to unobserved regions.

3.2 Partitioning of Terrestrial Water Storage Observations

Passive microwave (e.g., AMSR-E) retrievals have been used in conjunction with land surface models to better characterize snow (Sect. 3.1) and soil moisture (Sect. 3.4). Gravimetric measurements such as from GRACE can provide monthly, basin-scale ($>150,000$ km²) estimates of changes in TWS (Sect. 2.2). Since TWS is vertically integrated and includes groundwater, soil moisture, snow, and surface water, TWS retrievals offer significant insights into the regional- and continental-scale water balance and, through data assimilation, the potential to learn more about hydrological processes.

Besides the obvious spatial downscaling challenge presented by the basin-scale GRACE TWS retrievals, another challenge for the assimilation of GRACE-based TWS is the partitioning of the vertically integrated TWS retrievals into water cycle component variables. Like the horizontal downscaling of AMSR-E SWE retrievals discussed in the previous section, the partitioning of TWS retrievals can be accomplished through assimilation using an appropriate observation operator. In this case, the observation operator aggregates the fine-scale model estimates of soil moisture, groundwater, and snow to basin-scale TWS estimates. This observation operator enables the computation of the observation-minus-forecast residuals (or innovations) in the (basin-scale, TWS) space of the observations. The observation operator is also needed for the computation of the Kalman gain that transforms the innovations back into the space of the fine-scale model variables. Similarly, the required temporal aggregation of the model output to the monthly scale of the assimilated TWS retrievals is accomplished through the observation operator.

This concept was illustrated by Forman et al. (2012), who assimilated GRACE TWS retrievals over the Mackenzie River basin located in northwestern Canada (Fig. 3) using an updated version of the GEOS-5 LDAS developed by Zaitchik et al. (2008). The assimilation estimates were evaluated against independent SWE and river discharge observations (Sect. 2.3). Results suggest improved SWE estimates, including improved timing of the subsequent ablation and runoff of the snow pack. For example, Fig. 4 shows the improvements in SWE estimates resulting from the assimilation of GRACE TWS retrievals. The white bars represent model results without assimilation, whereas the gray bars represent results with assimilation. The labels on the y-axis of each subplot represent sub-basins of the Mackenzie River basin. As shown in Fig. 4, the assimilation of GRACE TWS retrievals generally reduced the mean difference and RMSE between the model and the independent CMC SWE estimates (Sect. 2.3). The reductions are greatest in the Liard basin, where the greatest amount of snow accumulation occurs. Here, the mean difference with the CMC estimates is reduced through GRACE data assimilation by 30 % (from 13.2 to 9.3 mm) and the RMSE is reduced by 18 % (from 24 to 19.6 mm). Smaller reductions occur in the other sub-basins. The correlation coefficient of the SWE anomalies (not shown) suggests a slight degree of degradation resulting from assimilation, but further analysis shows there is no statistically significant difference at the 5 % level. In summary, the assimilation of GRACE TWS information into the Catchment land surface model reduces the mean difference and RMSE in SWE estimates without adversely impacting estimates of interannual variability.

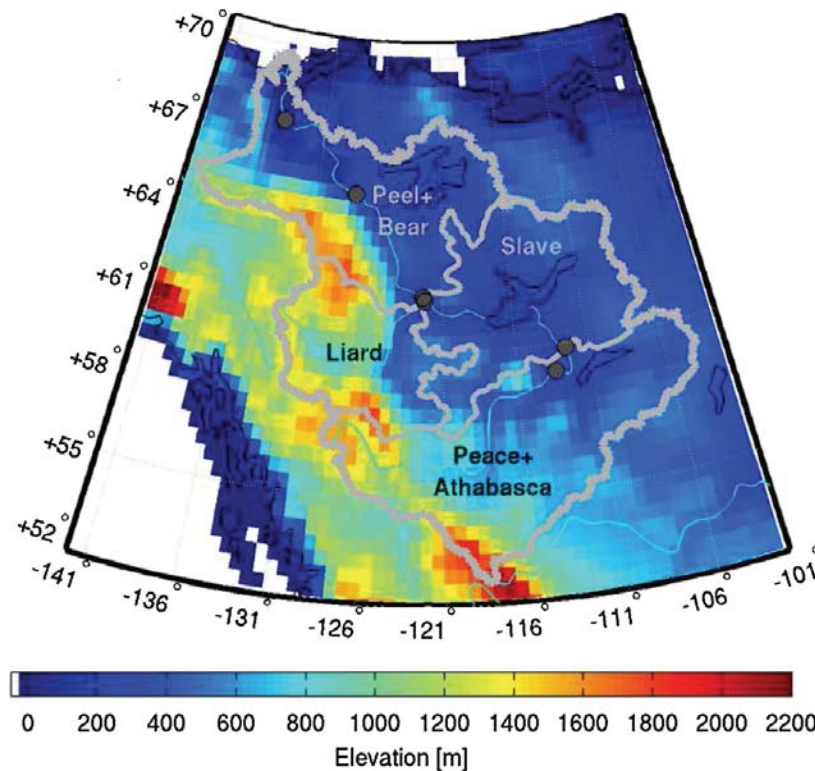


Fig. 3 Map of the 1,800,000 km² Mackenzie River Basin including GEOS-5 topography, sub-basin delineation, and GRDC observation locations (*solid dots*). Adapted from Forman et al. (2012)

Additional work was conducted to analyze modeled river discharge estimates against ground-based gauging stations. The findings (not shown) suggest that the assimilation of GRACE observations causes little or no change in the mean difference and RMSE of modeled river discharge, but that small, statistically significant improvements in the anomaly correlations were found. Improvements in the modeled river runoff anomalies are attributed to a redistribution of the water mass from the snow pack during the accumulation phase into the subsurface during the subsequent ablation and runoff phase. This redistribution of water by the assimilation framework effectively retains water within the hydrological basin for a longer period of time, which results in small but statistically significant improvements in modeled estimates of river discharge.

Investigation of the analysis increments can provide valuable insights into the behavior of the assimilation procedure and track how much and at what time water is being added to or removed from the individual TWS components. The thin, solid line in Fig. 5 shows the increments made to the subsurface water component. Averaged over the Mackenzie River basin and the 7-year experiment period, a total of 12.5 mm of water has been added into the subsurface by the assimilation procedure. This is most evident during the spring and summer. The thick, dashed line in Fig. 5 shows the increments for SWE. Averaged over time and space, SWE is removed during the accumulation phase with a small amount added back during the ablation and runoff phase for a total SWE increment of -45.1 mm. Acting together, the analysis increments to the subsurface water and SWE serve to reduce mass during snow accumulation and then increase the mass during ablation and runoff. These two phenomena essentially constrain the amplitude of the modeled TWS dynamics to achieve better agreement of the model estimates with the GRACE retrievals.

Fig. 4 SWE statistics of **a** mean difference and **b** RMSE for open loop (OL; *white*) and assimilation (DA; *light gray*) of GRACE TWS retrievals relative to CMC SWE estimates via Sturm et al. (2010). Statistics are for the Mackenzie River Basin (MRB) and its sub-basins Liard (L), Peace and Athabasca (P + A), Slave (S), and Bear and Peel (B + Pe) shown in Fig. 3. Adapted from Forman et al. (2012)

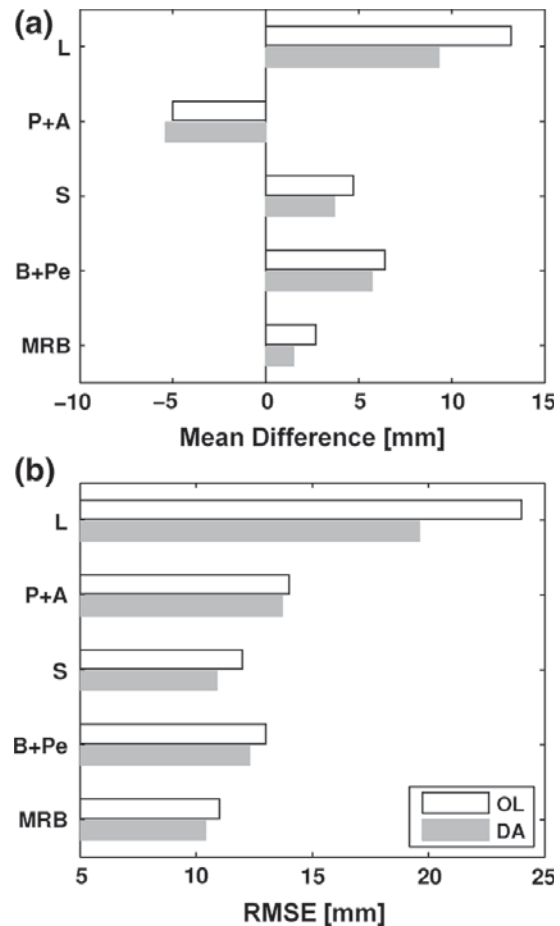
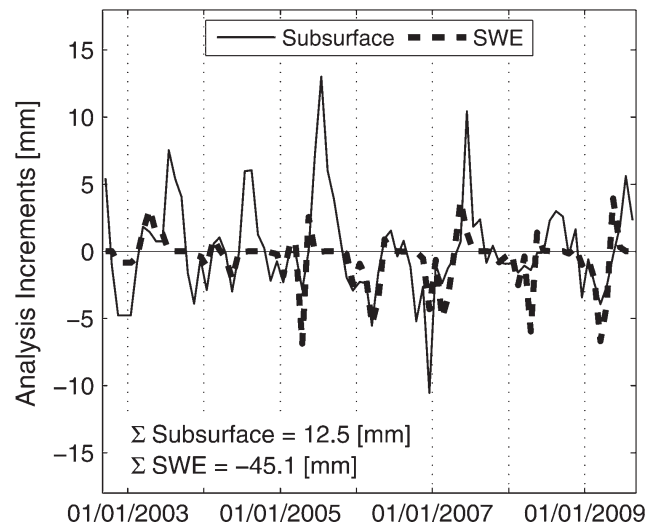


Fig. 5 Analysis increments for the entire Mackenzie River basin from GRACE TWS assimilation. The *thin, solid line* represents the subsurface water increments, whereas the *thick, dashed line* represents the SWE increments. Adapted from Forman et al. (2012)



The results shown in Figs. 4 and 5 imply that the assimilation procedure can effectively partition the vertically integrated GRACE TWS retrievals into their snow and subsurface water components. Houborg et al. (2012), Li et al. (2012), Su et al. (2010), and Zaitchik et al. (2008) further investigated the horizontal, vertical, and temporal disaggregation of GRACE TWS retrievals and reached similar conclusions for other basins in North America and Europe in different climate zones. Collectively, the growing body of research suggests

that GRACE TWS assimilation can lead to better understanding of the hydrological cycle in remote regions of the globe where ground-based observation collection is difficult, if not impossible. This information could ultimately lead to improved freshwater resource management as well as reduced uncertainty in river discharge.

3.3 Microwave Radiative Transfer Models for Radiance Data Assimilation

It is well established for atmospheric data assimilation systems that the assimilation of satellite radiance observations is preferable to the assimilation of geophysical retrievals (Eyre et al. 1993; Joiner and Dee 2000). The former approach incorporates the radiative transfer model into the assimilation system and thereby avoids inconsistencies in the use of ancillary data between the assimilation system and the (pre-processed) geophysical retrievals. For land data assimilation, however, the vast majority of publications assimilate geophysical retrievals (Lahoz and De Lannoy 2013). In this section, we discuss the development of forward radiative transfer models (RTMs) that convert land surface model variables into microwave brightness temperatures. The first example presents such a model for warm-season microwave brightness temperatures (Sect. 3.3.1). The second example introduces a neural network approach to predict microwave brightness temperatures over snow-covered land (Sect. 3.3.2).

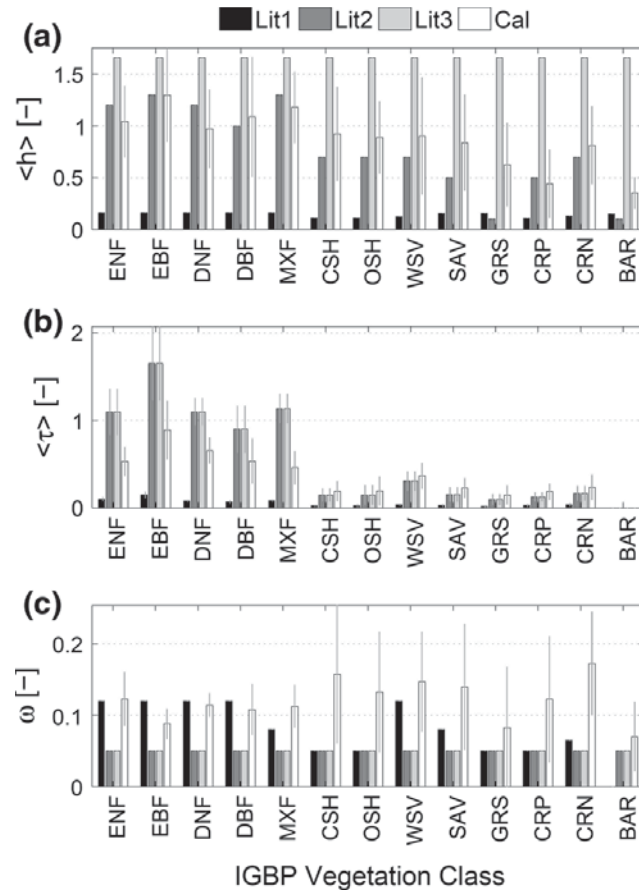
3.3.1 Warm-Season, L-Band Radiative Transfer Modeling

Global observations of brightness temperatures (T_b) at L-band (1.4 GHz) are available from the SMOS mission, and similar T_b observations are expected from the planned Soil Moisture Active Passive (SMAP; Entekhabi et al. 2010) mission. In preparation for the assimilation of T_b observations from SMOS and SMAP, De Lannoy et al. (2013) added a physically based, warm-season microwave RTM to the GEOS-5 Catchment model. The RTM is based on the commonly used, zero-order “tau-omega” approach that accounts for microwave emission by the soil and the vegetation canopy as well as attenuation by the vegetation. While the RTM is based on sound physical principles, determining the required parameter values for the microwave roughness, scattering albedo, and vegetation optical depth on a global scale is a serious challenge.

De Lannoy et al. (2013) collected three different sets of the literature values for the L-band RTM parameters. “Lit1” refers to parameters that are proposed for the future SMAP radiometer retrieval product, “Lit2” are parameters collected from the literature studies using the L-band Microwave Emission of the Biosphere model (Wigneron et al. 2007) and related models, and “Lit3” is the same as Lit2 except that the microwave roughness parameter is set to values used for SMOS monitoring in the European Centre for Medium-Range Weather Forecasts (ECMWF). The three sets of parameters are illustrated in Fig. 6, which shows the resulting microwave roughness (h), vegetation opacity (τ), and scattering albedo (ω) by vegetation class. As can be seen from the figure, there are large differences in h , τ , and ω between the three sets of the literature values. These differences translate into climatological differences in the simulated brightness temperatures.

For example, Fig. 7a–c shows the differences between 1-year mean (July 1, 2010–July 1, 2011) model simulations (using the three different literature-based sets of RTM parameters) and SMOS observations for H-polarized T_b at 42.5° incidence angle. Modeled brightness temperatures are at 36 km resolution, commensurate with the resolution of the SMOS observations. Brightness temperatures are screened for frozen soil conditions, snow on the ground, heavy precipitation, proximity to open water surfaces, and radio-frequency

Fig. 6 **a** Time-mean $\langle h \rangle$ (July 1, 2010–July 1, 2011), **b** time-mean $\langle \tau \rangle$, and **c** time-invariant ω ; (*Lit1*, *Lit2* and *Lit3*) before calibration, and (*Cal*) after calibration, spatially averaged by vegetation class. International Geosphere-Biosphere Program (*IGBP*) vegetation classes are (*ENF*) Evergreen Needleleaf Forest, (*EBF*) Evergreen Broadleaf Forest, (*DNF*) Deciduous Needleleaf Forest, (*DBF*) Deciduous Broadleaf Forest, (*MXF*) Mixed Forest, (*CSH*) Closed Shrublands, (*OSH*) Open Shrublands, (*WSV*) Woody Savannas, (*SAV*) Savannas, (*GRS*) Grasslands, (*CRP*) Croplands, (*CRN*) Cropland and Natural Vegetation, and (*BAR*) Barren or Sparsely Vegetated. Thin gray lines for *Cal* indicate the spatial standard deviation within each vegetation class. Adapted from De Lannoy et al. (2013)



interference. The figure shows that all three sets of the literature values for the RTM parameters lead to substantial biases against SMOS observations, with Lit1 being too cold (by 42.0 K on average) and Lit3 too warm (by 24.6 K on average). Even though Lit2 estimates are nearly unbiased in the global average, there are still significant regional biases in the simulated Tbs, with an average absolute bias of 12.7 K. Since such biases would interfere with the assimilation of satellite Tb, the RTM parameters need to be calibrated to achieve climatologically unbiased Tb simulations.

The most important RTM parameters determining h , τ , and ω have been calibrated, separately for each model grid cell, using multi-angular SMOS observations from July 1, 2011 to July 1, 2012. The calibration simultaneously minimizes, separately for each location, the difference between the modeled and observed climatological mean values, the difference between modeled and observed climatological standard deviations, and the deviations of the optimized parameters from prior guesses (that is, from Lit1, Lit2, or Lit3 values). Through investigating a number of calibration scenarios, De Lannoy et al. (2013) determined that it is best to simultaneously calibrate a subset of the RTM parameters that most directly determine h , τ , and ω .

After calibration, global Tb simulations for the validation year (July 1, 2010–July 1, 2011) are largely unbiased for multiple incidence angles and both H- and V-polarization. For example, Fig. 7d shows that the global average absolute bias is now just 2.7 K for H-polarized Tb at 42.5° incidence angle. It should be emphasized that an RMSE of approximately 10 K remains, which is partly due to seasonal biases and partly due to random errors. The former will be addressed in the assimilation system through bias estimation and correction, and the latter through the radiance-based soil moisture analysis.

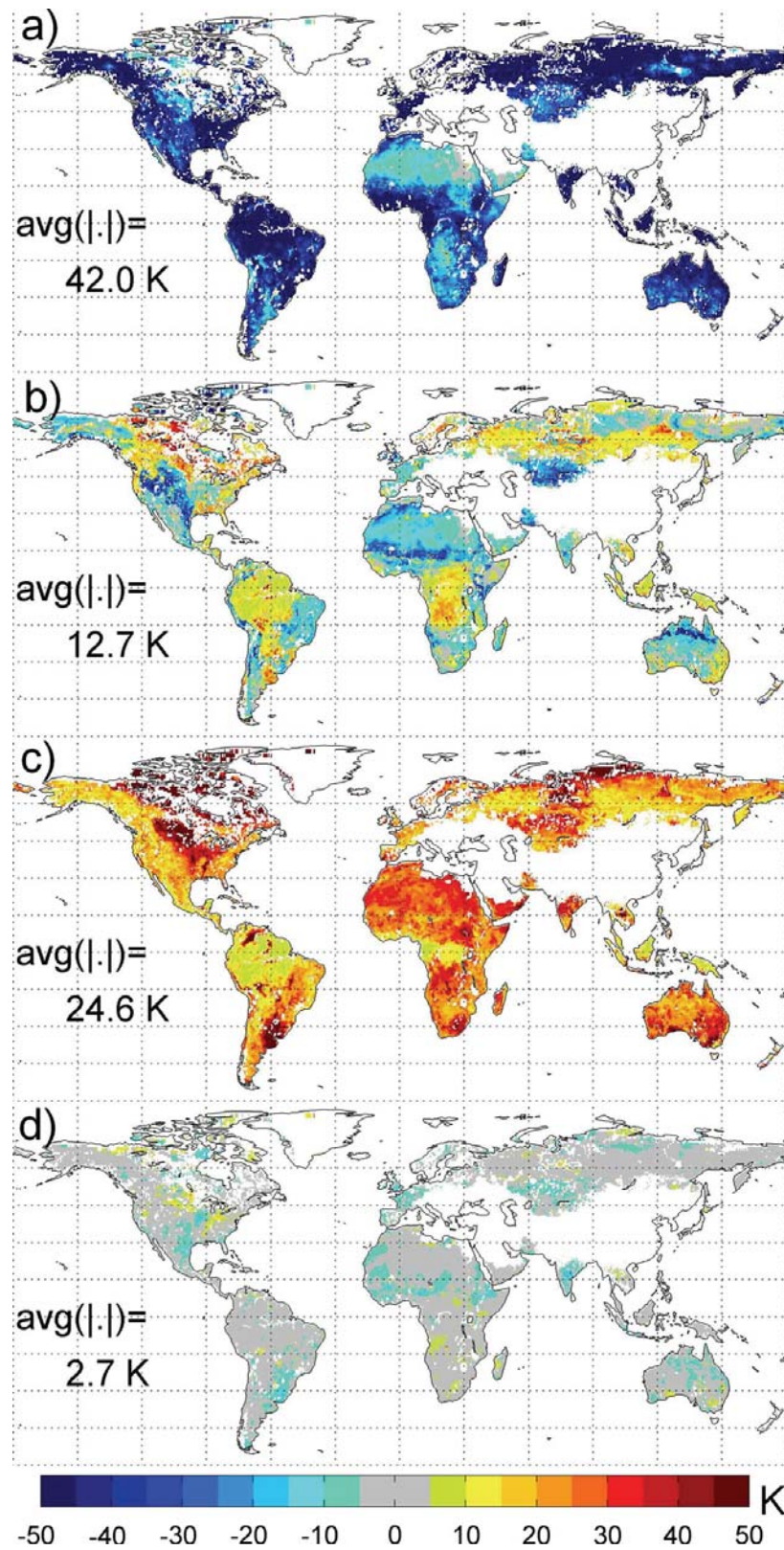


Fig. 7 Difference between 1-year (July 1, 2010–July 1, 2011) mean values of $Tb_H(42.5^\circ)$ in Kelvin from GEOS-5 and SMOS observations for **a** Lit1, **b** Lit2, **c** Lit3, and **d** calibrated parameters. Within each subplot, “avg(|.)” indicates the average absolute difference across the globe (excluding regions impacted by open water or radio-frequency interference that are shown in white). Adapted from De Lannoy et al. (2013)

The calibrated parameters are shown in Fig. 6. Results suggest, for example, that the roughness parameter (h) is too low in Lit1 and too high in Lit3. The calibrated vegetation opacity (τ) values distinguish clearly between high and low vegetation. The calibrated scattering albedo (ω) is increased over low vegetation, which reduces the vegetation effect in the simulated Tb. In summary, the climatological calibration generates plausible parameter values that are consistent with the underlying land modeling system.

3.3.2 Predicting Microwave Brightness Temperatures over Snow

As demonstrated in the previous section, the Catchment model (as do similar global land surface models) supports the application of a physically based microwave RTM for warm-season processes. However, the snow model components in global land surface models, including that in the Catchment model, are usually too simplistic to support physically based RTM modeling in the presence of snow. Specifically, global snow models lack reliable estimates of snow microphysical properties (such as grain size, ice layers, and depth hoar) which would be needed for physically based forward modeling of the microwave brightness temperatures. Forman et al. (2013) therefore constructed an empirical forward RTM for snow-covered land surfaces based on an Artificial Neural Network (ANN).

The Catchment model state variables used as input to the ANN include the density and temperature of the snowpack at multiple depths, the temperature of the underlying soil, the overlying air, and the vegetative canopy, and the total amount of water equivalent within the snowpack. In addition, a cumulative temperature gradient index (TGI) is used as a proxy for snow grain size evolution in the presence of a vapor pressure gradient. Using the above inputs, the ANN is trained and (independently) validated using 10.7, 18.7, and 36.5 GHz microwave brightness temperatures at H- and V-polarization from AMSR-E. The independent validation is accomplished as follows: From the 9-year AMSR-E data record, each single year is withheld in turn from the ANN training, and skill metrics for the resulting ANN predictions are computed only against the AMSR-E data that have been withheld from the ANN training.

Figure 8 demonstrates the performance of the ANN predictions relative to AMSR-E measurements that were not used during training. The figure illustrates the overall ability of the ANN to predict Tbs for the 10 GHz V-polarized channel. The ANN predictions are essentially unbiased (relative to the AMSR-E measurements) across the 9-year period (Fig. 8a). The RMSE is typically less than 5 K (Fig. 8b). In addition, the ANN demonstrates skill in predicting interannual variability, with anomaly R values well above 0.5 over large parts of North America (Fig. 8c). Relatively low skill can be seen in areas along the southern periphery, where the snowpack is relatively thin and ephemeral, as well as in areas north of the boreal forest, where sub-grid scale lake ice (which is not modeled in the land surface model) is common. In short, Fig. 8 suggests considerable skill by the ANN at predicting interannual variability in 10 GHz V-polarized Tbs across North America with negligible bias and a reasonable RMSE. The RMSE is somewhat higher but still reasonable (less than 10 K) for the higher frequencies and for H-polarization Tb (see Figures 4–6 of Forman et al. 2013).

Forman et al. (2013) also assessed the potential for using the ANN as a forward observation operator in radiance-based snow assimilation. For this demonstration, the observations are considered to be in the form of spectral differences in V-polarization brightness temperatures, $\Delta T_b \equiv T_{b_v}(18 \text{ GHz}) - T_{b_v}(36 \text{ GHz})$. Since ΔT_b typically increases with increasing SWE, this spectral difference is commonly used to estimate SWE

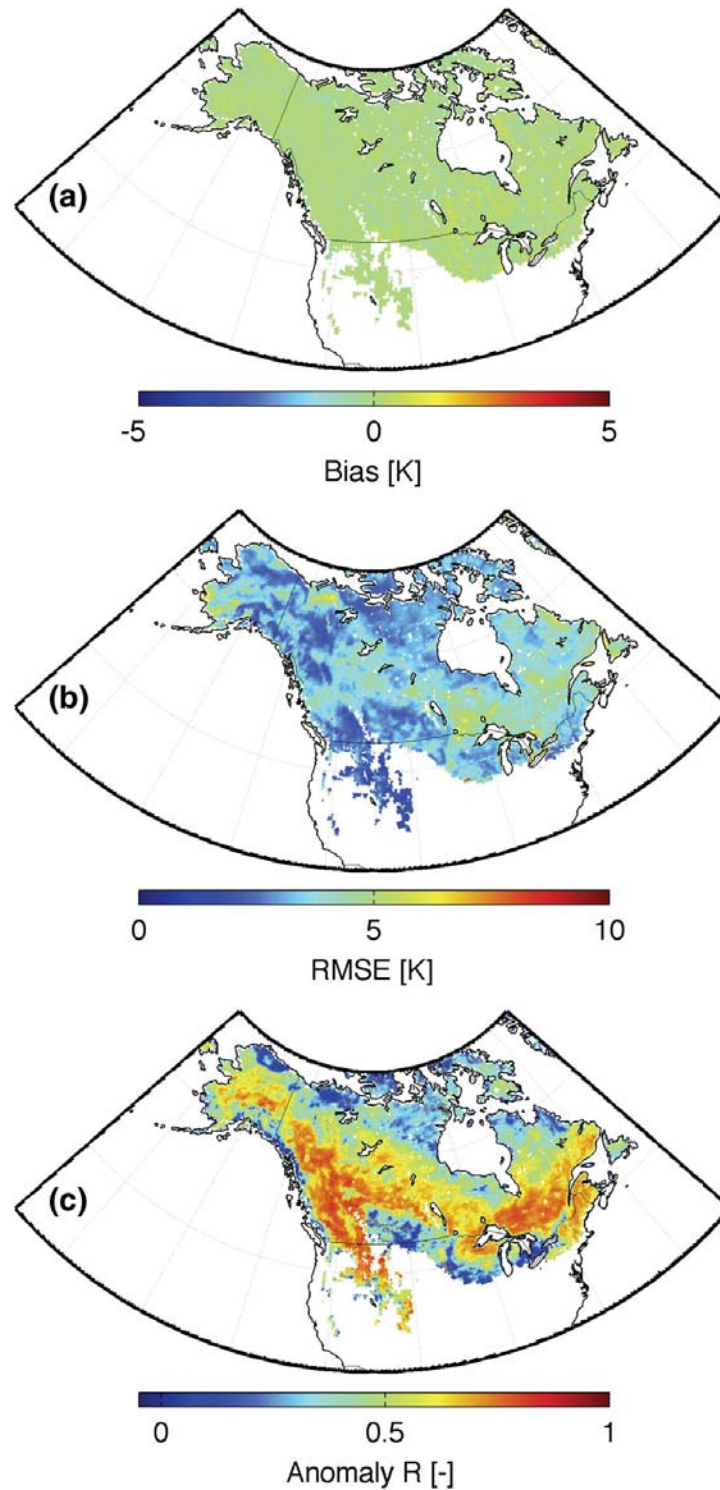


Fig. 8 **a** Bias, **b** RMSE, and **c** anomaly R for ANN simulated 10 GHz V-polarized T_b from September 1, 2002 to September 1, 2011 versus AMSR-E observations not used in training. Anomaly R values not statistically different from zero at the 95 % significance level based on a Fisher Z transform are shown in gray. Such non-significant R values occur in only a few very small regions

in retrieval algorithms (Kelly 2009). For the demonstration of the radiance-based assimilation considered here, observations of ΔT_b imply that the resulting Kalman gain is proportional to error correlations between modeled SWE and ANN predictions of ΔT_b . To

obtain analysis increments, the Kalman gain would be multiplied with innovations in ΔT_b (that is, the difference between actual AMSR-E observations of ΔT_b and ANN predictions of ΔT_b).

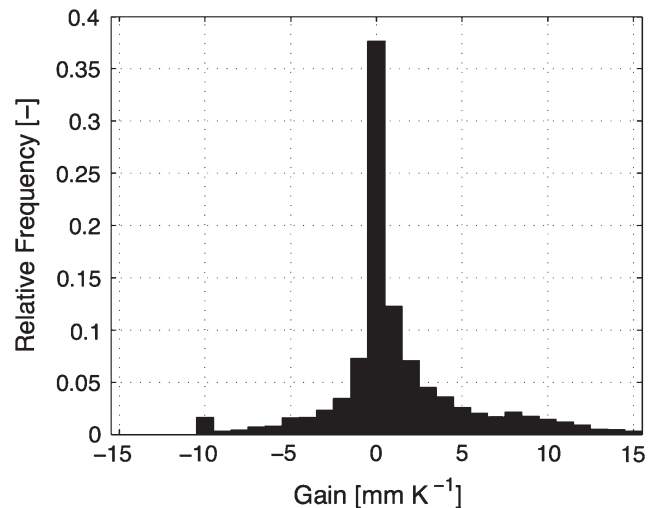
The Kalman gain computed for February 6, 2003 ranges from -10 to 15 mm K^{-1} as illustrated in Fig. 9. A gain of 1 mm K^{-1} equates to an increase of 1 mm in the posterior (updated) modeled SWE for a 1 K innovation (that is, for a difference of 1 K between AMSR-E ΔT_b measurements and ANN ΔT_b predictions). Similarly, a negative Kalman gain in the presence of a positive-valued innovation would equate to a reduction in modeled SWE. Most importantly, the results suggest that there is a nonzero error correlation between the model SWE forecasts and the simulated ΔT_b measurements across much of the North American domain. Overall, the results suggest that the ANN could serve as a computationally efficient observation operator for radiance-based snow data assimilation at the continental scale.

3.4 Observation Selection for a Root Zone Soil Moisture Analysis

Knowledge of the amount of moisture stored in the root zone of the soil is important for many applications related to the transfer of water, energy, and carbon between the land and the atmosphere, including the assessment, monitoring, and prediction of drought (Senviratne et al. 2010). At the global scale, soil moisture estimates are usually based on two sources of information: (1) direct observations of surface soil moisture from satellite and (2) observation-based precipitation forcing driving a numerical model of soil moisture dynamics. However, neither surface soil moisture retrievals nor precipitation observations provide direct measurements of soil moisture in the root zone. The selection of the most relevant types of observations for a root zone soil moisture analysis therefore presents an important conceptual problem.

A priori, it is not obvious whether the estimation of root zone soil moisture would benefit more from the use of precipitation observations (as, for example, in the Global Land Data Assimilation System; Rodell et al. 2003) or from the assimilation of surface soil moisture retrievals (as, for example, illustrated by Reichle et al. 2007). This section provides examples of both approaches. First, a land surface reanalysis that relies on observed precipitation is presented, followed by a root zone soil moisture analysis that is based on the assimilation of surface soil moisture retrievals. Finally, the two sources of soil moisture

Fig. 9 Histogram of the Kalman gain on February 6, 2003 for SWE versus $\Delta T_b = [T_{b_V}(18 \text{ GHz}) - T_{b_V}(36 \text{ GHz})]$



information are merged and compared directly in a single system, and their relative contributions to the skill of root zone soil moisture estimates are assessed.

3.4.1 Using Precipitation Observations

The Modern-Era Retrospective Analysis for Research and Applications (MERRA) is a state-of-the-art atmospheric reanalysis data product based on GEOS-5 that provides, in addition to atmospheric fields, global estimates of soil moisture, latent heat flux, snow, and runoff for 1979—present with a latency of about 1 month (Rienecker et al. 2011). A supplemental and improved set of land surface hydrological fields (“MERRA-Land”) is generated routinely using an improved version of the land component of the MERRA system (Reichle et al. 2011; Reichle 2012). Specifically, the MERRA-Land estimates benefit from corrections to the MERRA precipitation forcing with the global gauge-based NOAA Climate Prediction Center “Unified” (CPCU) precipitation product and from revised parameter values in the rainfall interception model, changes that effectively correct for known limitations in the MERRA surface meteorological forcings.

With a few exceptions, the MERRA-Land data appear more accurate than the original MERRA estimates and are thus recommended for those interested in using MERRA output for land surface hydrological studies. As an example, Fig. 10 examines the drought conditions experienced across the western United States and along the East Coast. The MERRA and MERRA-Land drought indicator shown in the figure is derived by ranking, separately for each grid cell, the normalized, monthly mean root zone soil moisture anomalies for June, July, and August of 1980 through 2011 and converting the rank into percentile units. For comparison, the drought severity assessed independently by U.S. Drought Monitor is also shown. The figure clearly demonstrates that MERRA-Land data are more consistent with the Drought Monitor than MERRA data.

Reichle et al. (2011) and Reichle (2012) provide a more comprehensive and quantitative analysis of the skill (defined as the correlation coefficient of the anomaly time series with independent observations) in land surface hydrological fields from MERRA, MERRA-Land, and the latest global atmospheric reanalysis produced by ECWMF (ERA-I; Dee et al. 2011). Figure 11 shows that MERRA-Land and ERA-I root zone soil moisture skills (against in situ observations at 85 US stations) are comparable and significantly greater than that of MERRA. Furthermore, the runoff skill (against naturalized stream flow observations from 18 US basins) of MERRA-Land is typically higher than that of MERRA and ERA-I (not shown). Throughout the northern hemisphere, MERRA and MERRA-Land agree reasonably well with in situ snow depth measurements (from 583 stations) and with SWE from an independent analysis (not shown). In summary, through observations-based corrections of the MERRA precipitation forcing, MERRA-Land provides a supplemental and significantly improved land surface reanalysis product.

3.4.2 Assimilating Surface Soil Moisture Retrievals

Satellite retrievals of surface soil moisture are not used in MERRA-Land but would almost certainly have further improved the skill of root zone soil moisture estimates. Draper et al. (2012) illustrate the potential gains from assimilating ASCAT (Bartalis et al. 2007; Wagner et al. 1999) and 10.7 GHz AMSR-E Land Parameter Retrieval Model (LPRM; de Jeu et al. 2008) surface soil moisture retrievals. The retrievals are assimilated, both separately and jointly, over 3.5 years into the GEOS-5 LDAS, using MERRA forcing and initial conditions. Soil moisture skill is measured as the anomaly time series correlation coefficient

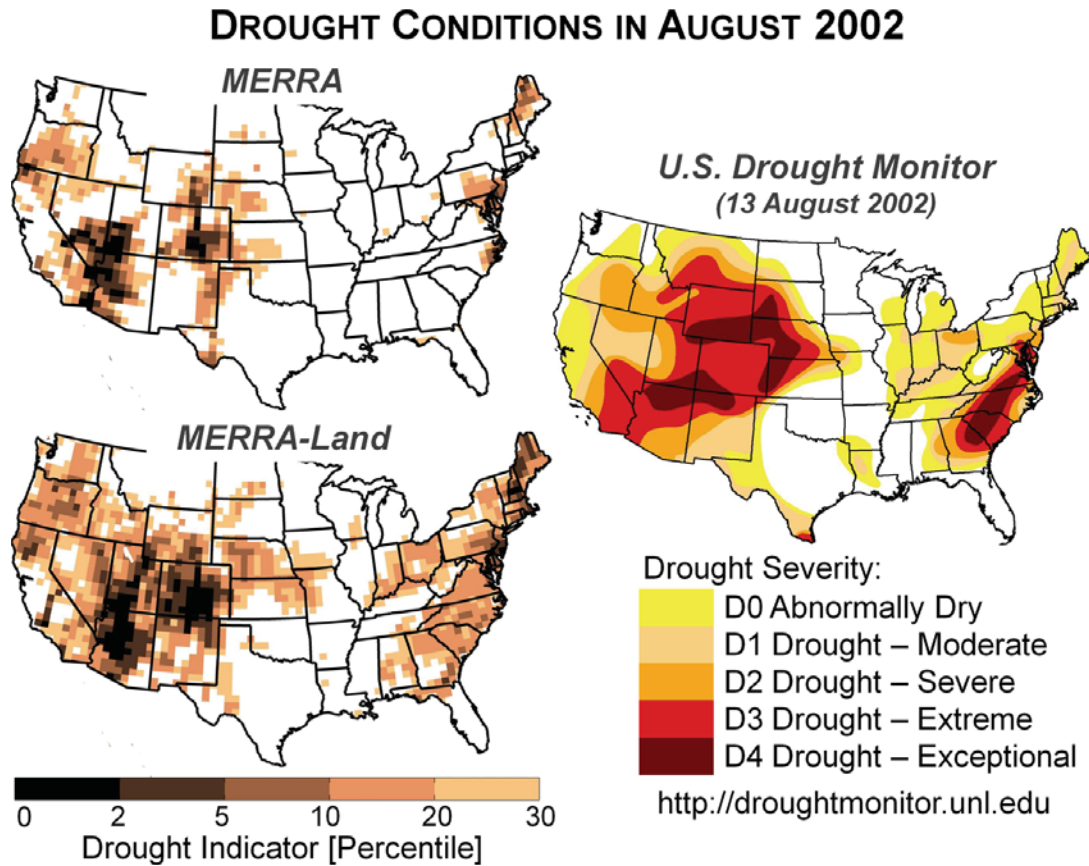
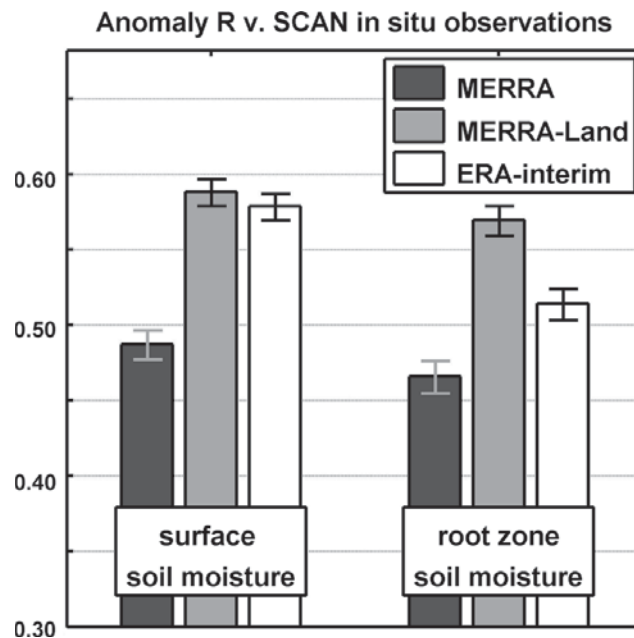


Fig. 10 Drought indicator derived from (top left) MERRA and (bottom left) MERRA-Land root zone soil moisture estimates for August 2002. Darker colors indicate more severe drought conditions. MERRA-Land estimates are more consistent than MERRA estimates with an independent drought assessment from the US Drought Monitor for August 13, 2002 (right)

Fig. 11 Skill (pentad anomaly R ; dimensionless) of MERRA, MERRA-Land, and ERA-I estimates (2002–2009) versus SCAN in situ surface and root zone soil moisture measurements at 85 stations. Error bars indicate approximate 95 % confidence intervals. Adapted from Reichle (2012)



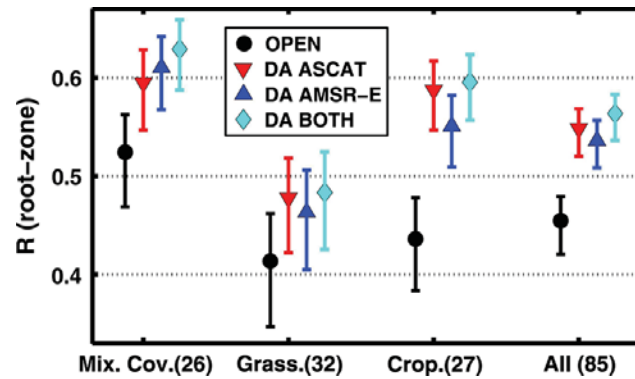


Fig. 12 Mean skill for root zone soil moisture from the open loop (ensemble mean, no assimilation), and the data assimilation (DA) of ASCAT, AMSR-E, and both surface soil moisture retrievals, averaged by land cover class, with 95 % confidence intervals. The number of sites in each land cover class is given in the axis labels. Skill is defined as the daily anomaly R value versus SCAN/SNOTEL and Murrumbidgee in situ observations. Adapted from Draper et al. (2012)

(R) with in situ soil moisture observations from the SCAN/SNOTEL network in the US (66 sites) and the Murrumbidgee Soil Moisture Monitoring Network in Australia (19 sites). These 85 sites are surrounded by terrain with low topographic complexity based on data provided with the ASCAT observations. Averaged over these sites, the ASCAT and AMSR-E surface soil moisture retrievals have similar skill (Draper et al. 2012).

Figure 12 shows the estimated R values and their 95 % confidence intervals for root zone soil moisture from the assimilation of ASCAT, AMSR-E, and both. The results are benchmarked against an open loop (no assimilation) model integration and have been averaged by land cover type (based on MODIS land cover classifications). Averaged across all 85 sites, assimilating ASCAT and/or AMSR-E surface soil moisture retrievals significantly improved the root zone soil moisture skill (at the 5 % level). The mean skill was increased from 0.45 for the open loop, to 0.55 for the assimilation of ASCAT, 0.54 for the assimilation of AMSR-E, and 0.56 for the assimilation of both.

Assimilating the ASCAT or AMSR-E retrievals also improved the mean R value over each individual land cover type, in most cases significantly. At the frequencies observed by AMSR-E and ASCAT, dense vegetation limits the accuracy of soil moisture observations, and so the improvements obtained over the mixed cover sites, which have 10–60 % trees or wooded vegetation, are very encouraging. For each land cover type, the skill obtained from the assimilation of ASCAT or AMSR-E retrievals was very similar. The combined assimilation of ASCAT and AMSR-E retrievals generally matched or slightly exceeded the mean R values from the single-sensor assimilation experiments.

Draper et al. (2012) also examined the contribution of the model skill and the observation skill to the skill of the assimilation estimates. The color surface in Fig. 13 shows the skill improvements (ΔR) in root zone soil moisture, where ΔR is defined as the skill (R) of the assimilation estimates (from the single-sensor assimilation of ASCAT or AMSR-E retrievals) minus that of the open loop model estimates. The skill improvements are shown as a function of the open loop model skill and the retrieval skill. Specifically, the ordinate measures the skill of the open loop root zone soil moisture estimates, and the abscissa measures the skill of the assimilated (ASCAT or AMSR-E) surface soil moisture retrievals. Where the skill of the assimilated retrievals is no more than 0.2 less than the open loop skill (below the dashed line), the assimilation improves the root zone soil moisture skill. The improvements increase (up to 0.4) as the observation skill increases relative to that of the

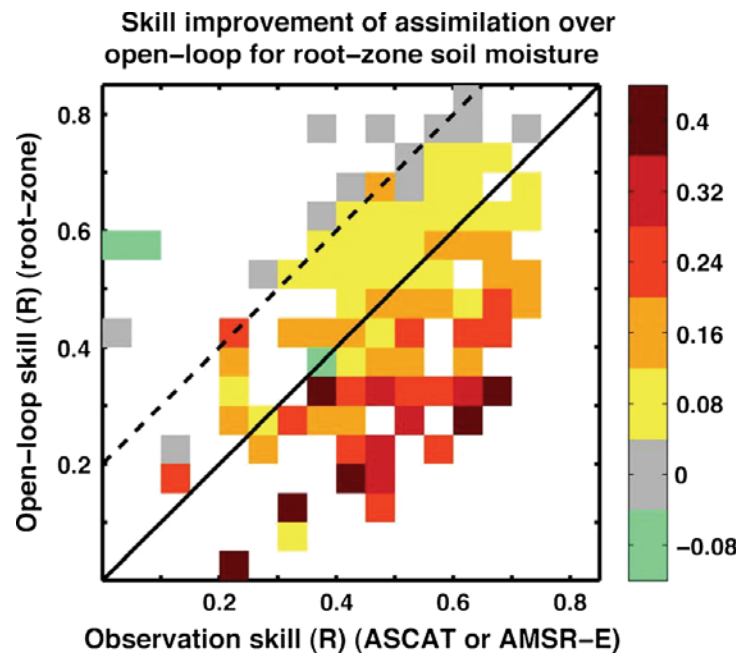


Fig. 13 Root zone soil moisture skill improvement (ΔR) from assimilating either ASCAT or AMSR-E surface soil moisture retrievals as a function of (ordinate) the open loop model skill and (abscissa) the observation skill. Skill improvement (ΔR) is defined as the skill of the assimilation product minus the open loop skill, with skill based only on days with data available from both satellites. Skill is assessed versus in situ measurements from the SCAN and Murrumbidgee networks. Significant improvements are found in the area below the dashed line where the skill of the retrievals may be lower than that of the open loop by up to 0.2. Adapted from Draper et al. (2012)

open loop (toward the bottom right hand corner). (The results are very similar if the ordinate measures surface soil moisture skill; not shown). Figure 13 thus provides a practical demonstration of the minimum skill required for soil moisture observations to be beneficial in a land data assimilation system and confirms the findings obtained by Reichle et al. (2008b) using synthetically generated observations. In summary, the assimilation of active or passive microwave data significantly improves the model root zone soil moisture estimates by a similar amount, even in cases where the assimilated surface soil moisture retrievals are less skillful than the open loop soil moisture estimates.

3.4.3 Combining Precipitation Observations and Surface Soil Moisture Retrievals

Liu et al. (2011a) used both precipitation observations and surface soil moisture retrievals within the GEOS-5 LDAS and investigated their relative contributions to the skill of root zone soil moisture estimates. Relative to baseline soil moisture estimates from MERRA, their study investigates soil moisture skill derived from (1) land model forcing corrections based on large-scale, gauge-, and satellite-based precipitation observations and (2) assimilation of surface soil moisture retrievals from AMSR-E. Three precipitation products were used (separately) to correct the MERRA precipitation toward gauge- and satellite-based observations: the NOAA Climate Prediction Center Merged Analysis of Precipitation (CMAP) pentad product (“standard” version), the Global Precipitation Climatology Project (GPCP) version 2.1 pentad product, and the NOAA Climate Prediction Center (CPC) daily unified precipitation analysis over the United States.

Two different surface soil moisture retrieval products were assimilated into the GEOS-5 LDAS: (1) the operational NASA Level-2B AMSR-E “AE-Land” product (version V09) archived at the National Snow and Ice Data Center (NSIDC; Njoku et al. 2003) and (2) the AMSR-E LPRM product (de Jeu et al. 2008). Soil moisture skill is assessed using in situ observations in the continental United States at the 37 single-profile sites within the SCAN network for which skillful AMSR-E retrievals are available. As in Sect. 3.4.2, skill is assessed in terms of the anomaly time series correlation coefficient R .

Figure 14 shows comparable average skill for surface soil moisture estimates from the two AMSR-E products and from the Catchment model with MERRA precipitation forcing without data assimilation. Consistent with the findings of Sect. 3.4.1, adding information from precipitation observations increases soil moisture skills for surface and root zone soil moisture. Consistent with the results of Sect. 3.4.2, assimilating satellite estimates of surface soil moisture also increases soil moisture skills, again for surface and root zone soil moisture. The salient result is that adding information from both sources (precipitation observations and surface soil moisture retrievals) increases soil moisture skills by almost the sum of the individual skill contributions, which demonstrates that precipitation corrections and assimilation of satellite soil moisture retrievals contribute important and largely independent amounts of information.

Liu et al. (2011a) also repeated their skill analysis against measurements from four USDA Agricultural Research Service (“CalVal”) watersheds with high-quality distributed sensor networks that measure surface soil moisture at the scale of land model and satellite

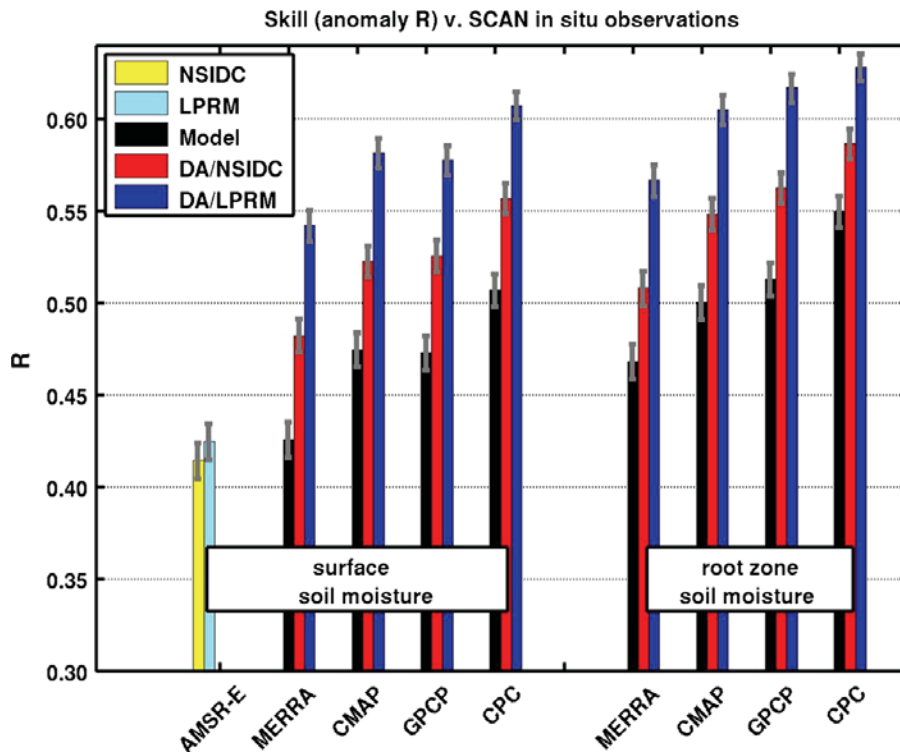


Fig. 14 Skill (daily anomaly R ; dimensionless) versus SCAN in situ soil moisture measurements for estimates from two AMSR-E retrieval datasets (NSIDC and LPRM), the Catchment model forced with four different precipitation datasets (MERRA, CMAP, GPCP, and CPC), and the corresponding data assimilation integrations (red bars: DA/NSIDC and blue bars: DA/LPRM). Average is based on 37 SCAN sites for surface and 35 SCAN sites for root zone soil moisture. Error bars indicate approximate 95 % confidence. Adapted from Liu et al. (2011a)

estimates (Jackson et al. 2010). As expected, the skill of the satellite, model, and assimilation estimates is higher when it is assessed against the multi-sensor CalVal observations rather than against single-profile SCAN measurements (not shown). The relative skill contributions by precipitation corrections and soil moisture retrieval assimilation, however, remain unchanged (not shown). This corroborates the results shown in Fig. 14 which were obtained with a larger network of single-profile sensors.

Taken together, the results of this section strongly suggest that future land surface reanalysis efforts would benefit from the use of both precipitation observations and satellite retrievals of surface soil moisture because both types of observations contribute significant and largely independent amounts of information to the skill of root zone soil moisture in the analysis. Moreover, both active and passive surface soil moisture retrievals should be assimilated for maximum coverage and accuracy.

4 Summary and Discussion

The present study discussed several conceptual challenges in land surface hydrological data assimilation as part of an effort toward improving our understanding of the Earth's hydrological cycle (Trenberth and Asrar 2013). The challenges arise from a seeming mismatch between the assimilated observations and the water cycle variables of interest that can be overcome through the careful design of the assimilation system. This was illustrated with examples from recent research findings using the GEOS-5 LDAS.

The first challenge is the use of coarse-scale satellite observations to estimate land surface fields at finer scales of interest. Such horizontal downscaling can be accomplished by using a fine-scale land surface model and by defining an observation operator that maps from the fine-scale model space to the space of the coarse-scale observations (Sect. 3.1). In the presence of larger-scale model error correlations, the assimilation system can also spread observational information to unobserved locations.

The second challenge is the partitioning of satellite observations (such as TWS retrievals) into their component variables. This partitioning can again be accomplished through an observation operator. In the case of TWS assimilation, the observation operator maps from the fine-scale model estimates of soil moisture and snow to basin-scale TWS (Sect. 3.2). The observation operator therefore enables the computation of the observation-minus-forecast residuals (innovations). The observation operator is also needed for the computation of the Kalman gain matrix that transforms the observation-space (coarse-scale TWS) innovations into the model-space (fine-scale soil moisture and snow) analysis increments.

The third challenge is the development of microwave RTMs for use as observation operators in radiance-based data assimilation. Two examples were given. In the first example, a global microwave RTM for warm-season, L-band brightness temperatures was calibrated successfully using SMOS observations (Sect. 3.3.1). In the second example, an empirical approach based on an artificial neural network yielded robust model simulations of AMSR-E microwave brightness temperatures over snow-covered land at continental scales (Sect. 3.3.2). In both cases, the results are very encouraging and constitute progress toward replacing the commonly used assimilation of geophysical retrievals (such as SWE or surface soil moisture retrievals) with the direct assimilation of satellite radiances. Note that a radiance-based soil moisture analysis can partition the observational (brightness temperature) information into increments of model soil moisture, soil temperature, and vegetation water content (essentially, the model variables that most impact the brightness temperature). In other words, the microwave RTM, acting as the observation operator,

takes on a role that is conceptually similar to that of the observation operator used for the partitioning of TWS information into its water cycle components (Sect. 3.2).

The fourth and final challenge addressed in the paper discusses the selection of the types of observations that are most relevant for the analysis of poorly observed variables. For the analysis of one such variable, root zone soil moisture, the use of gauge- and satellite-based precipitation observations along with active and passive surface soil moisture retrievals was investigated (Sect. 3.4). It was shown that the MERRA-Land surface reanalysis provides better estimates of root zone soil moisture than MERRA due to the use of gauge-based precipitation observations in MERRA-Land. Next, the potential skill gained from the assimilation of surface soil moisture retrievals was investigated. It was demonstrated that improved root zone soil moisture estimates can be obtained even where the skill of the assimilated surface soil moisture retrievals is somewhat poorer than that of the model estimates of surface soil moisture. For maximum coverage and accuracy, both active and passive retrievals should be assimilated. Finally, it was shown that the use of precipitation observations and the assimilation of surface soil moisture retrievals contribute significant and largely independent amounts of root zone soil moisture information. Therefore, future reanalyses should use both of these observation types. This finding is consistent with the general expectation that using more observations in a data assimilation system will improve its output.

In some cases (for example, Sects. 3.1 and 3.2), the appropriate observation operator and assimilation system configuration entail that neighboring grid cells (or land model tiles) are no longer computationally independent in the assimilation system, even if they are independent in the land model (Reichle and Koster 2003). These computational dependencies arise through spatially correlated perturbation fields or spatially distributed analysis update calculations. Such “three-dimensional” land data assimilation systems therefore necessitate greater computational resources than more simplistic, “one-dimensional” assimilation systems where all model grid cells (or tiles) are treated independently. It is assumed here that the purely technical challenge of computational demand can be overcome with sophisticated software engineering and the increasing availability of affordable and massively parallel computing architectures.

5 Conclusions and Outlook

The present paper focused on the seeming mismatch between satellite observations and the water cycle variables of interest, and how a mismatch can be overcome through careful design and application of a land data assimilation system. Responding to the challenge questions of Sect. 1, we find that, if designed properly, a land data assimilation system can enable

1. the horizontal downscaling of coarse-scale satellite observations,
2. the partitioning of vertically integrated satellite measurements such as TWS into their water cycle components,
3. the direct assimilation of satellite radiances for soil moisture or snow analyses, and
4. the propagation of information from observed fields such as precipitation and surface soil moisture into variables such as root zone soil moisture, that are of great interest but are not directly observed by satellites.

Naturally, many challenges still lie ahead. State-of-the-art land data assimilation algorithms are only now emerging in operational systems. Much of the recent progress has

been achieved in so-called “off-line” (land-only) assimilation systems. These advances need to be incorporated into the coupled land–atmosphere systems used in atmospheric data assimilation and numerical weather prediction (NWP). Ground-breaking advances in coupled land–atmosphere data assimilation are being made, for example, at ECMWF (de Rosnay et al. 2012a, b). At the same time, the coupling of the GEOS-5 LDAS to the GEOS-5 atmospheric data assimilation system is underway at the NASA GMAO.

Moreover, much of the progress in land data assimilation has been with systems that assimilate only one type of observation, often surface soil moisture. In future, more emphasis will need to be placed on the assimilation of multiple types of observations within a single assimilation system, including observations of water cycle components such as soil moisture, SWE, snow cover fraction, TWS, and precipitation.

Future development should also address the addition or improvement of runoff routing and surface water storage model components in the global land surface models used in NWP. The planned NASA Surface Water and Ocean Topography (SWOT; Durand et al. 2010) mission, for instance, will provide high-resolution observations of surface water elevation. To improve our understanding of the global hydrological cycle, it will be crucial to incorporate these new observations into global land data assimilation systems, building on early studies such as those by Andreadis et al. (2007), Biancamaria et al. (2011), and Durand et al. (2008).

Finally, the existing global land data assimilation systems will need to consider the modeling of vegetation dynamics and the assimilation of current or planned satellite observations such as the Fraction of Absorbed Photosynthetically Active Radiation (FAPAR), the Leaf Area Index (LAI), or the multi-angular Photochemical Reflectance Index (PRI) (Albergel et al. 2010; Hilker et al. 2012; Kaminski et al. 2012; Knorr et al. 2010; Muñoz Sabater et al. 2008; Stöckli et al. 2011). Furthermore, current microwave sensors already provide observations of the freeze–thaw state of the landscape at coarse scales (Kim et al. 2010), and SMAP will provide much higher-resolution observations with continental coverage (Entekhabi et al. 2010). These vegetation and freeze–thaw observations link the hydrological and carbon cycles and should be used in global land data assimilation systems.

Acknowledgments The authors thank the organizers of the ISSI Workshop on “The Earth’s Hydrological Cycle” held February 6–10, 2012 and two anonymous reviewers for their efforts. The research was supported by the NASA program on The Science of Terra and Aqua, the NASA Soil Moisture Active Passive mission, the NASA Postdoctoral Program, and the NASA High-End Computing program.

References

- Albergel C, Calvet J-C, Mahfouf J-F, Rüdiger C, Barbu AL, Lafont S, Roujean J-L, Walker JP, Crapeau M, Wigneron J-P (2010) Monitoring of water and carbon fluxes using a land data assimilation system: a case study for southwestern France. *Hydrol Earth Syst Sci* 14:1109–1124. doi:10.5194/hess-14-1109-2010
- Andreadis K, Lettenmaier D (2006) Assimilating remotely sensed snow observations into a macroscale hydrology model. *Adv Water Resour* 29:872–886
- Andreadis KM, Clark EA, Lettenmaier DP, Alsdorf DE (2007) Prospects for river discharge and depth estimation through assimilation of swath-altimetry into a raster-based hydrodynamics model. *Geophys Res Lett* 34:L10403. doi:10.1029/2007GL029721
- Barnett TP, Adam JC, Lettenmaier DP (2005) Potential impacts of a warming climate on water availability in snow-dominated regions. *Nature* 438:303–309. doi:10.1038/nature04141
- Bartalis Z, Wagner W, Naeimi V, Hasenauer S, Scipal K, Bonekamp H, Figa J, Anderson C (2007) Initial soil moisture retrievals from the METOP-A Advanced Scatterometer (ASCAT). *Geophys Res Lett* 34:L20401. doi:10.1029/2007GL031088

- Biancamaria S, Durand M, Andreadis KM, Bates PD, Boone A, Mognard NM, Rodríguez E, Alsdorf DE, Lettenmaier DP, Clark EA (2011) Assimilation of virtual wide swath altimetry to improve Arctic river modeling. *Remote Sens Environ* 115:373–381. doi:[10.1016/j.rse.2010.09.008](https://doi.org/10.1016/j.rse.2010.09.008)
- Brasnett B (1999) A global analysis of snow depth for numerical weather prediction. *J Appl Meteorol* 38:726–740
- Brown RD, Brasnett B (2010) Canadian Meteorological Centre (CMC) daily snow depth analysis data. Environment Canada, Boulder, Colorado, National Snow and Ice Data Center, available at http://nsidc.org/data/docs/daac/nsidc0447_CMC_snow_depth
- Bruinsma S, Lemoine J-M, Biancale R, Vales N (2010) CNES/GRGS 10-day gravity field models (release 2) and the evaluation. *Adv Space Res* 45:587–601
- Clifford D (2010) Global estimates of snow water equivalent from passive microwave instruments: history, challenges, and future developments. *Int J Remote Sens* 31:3707–3726
- Crow WT, Reichle RH (2008) Comparison of adaptive filtering techniques for land surface data assimilation. *Water Resour Res* 44:W08423. doi:[10.1029/2008WR006883](https://doi.org/10.1029/2008WR006883)
- Crow WT, van den Berg MJ (2010) An improved approach for estimating observation and model error parameters for soil moisture data assimilation. *Water Resour Res* 46:W12519. doi:[10.1029/2010WR009402](https://doi.org/10.1029/2010WR009402)
- Crow WT, Wood EF (2003) The assimilation of remotely sensed soil brightness temperature imagery into a land surface model using ensemble Kalman filtering: a case study based on ESTAR measurements during SGP97. *Adv Water Resour* 26:137–149
- de Jeu RAM, Wagner W, Holmes TRH, Dolman AJ, Giesen NC, Friesen J (2008) Global soil moisture patterns observed by space borne microwave radiometers and scatterometers. *Surv Geophys* 29:399–420. doi:[10.1007/s10712-008-9044-0](https://doi.org/10.1007/s10712-008-9044-0)
- De Lannoy GJM, Reichle RH, Houser PR, Pauwels VRN, Verhoest NEC (2007) Correcting for forecast bias in soil moisture assimilation with the ensemble Kalman filter. *Water Resour Res* 43:W09410. doi:[10.1029/2006WR005449](https://doi.org/10.1029/2006WR005449)
- De Lannoy GJM, Reichle RH, Houser PR, Arsenault KR, Verhoest NEC, Pauwels VRN (2010) Satellite-scale snow water equivalent assimilation into a high-resolution land surface model. *J Hydrometeorol* 11:352–369. doi:[10.1175/2009JHM1192.1](https://doi.org/10.1175/2009JHM1192.1)
- De Lannoy GJM, Reichle RH, Arsenault KR, Houser PR, Kumar SV, Verhoest NEC, Pauwels VRN (2012) Multi-scale assimilation of AMSR-E snow water equivalent and MODIS snow cover fraction in northern Colorado. *Water Resour Res* 48:W01522. doi:[10.1029/2011WR010588](https://doi.org/10.1029/2011WR010588)
- De Lannoy GJM, Reichle RH, Pauwels VRN (2013) Global calibration of the GEOS-5 L-band microwave radiative transfer model over land using SMOS observations. *J Hydrometeorol*. doi:[10.1175/JHM-D-12-092.1](https://doi.org/10.1175/JHM-D-12-092.1)
- de Rosnay P, Drusch M, Vasiljevic D, Balsamo G, Albergel C, Isaksen L (2012a) A simplified extended Kalman filter for the global operational soil moisture analysis at ECMWF. *Q J R Meteorol Soc*. doi:[10.1002/qj.2023](https://doi.org/10.1002/qj.2023)
- de Rosnay P, Balsamo G, Albergel C, Munoz Sabater J, Isaksen L (2012b) Initialisation of land surface variables for numerical weather prediction. *Surv Geophys*. doi:[10.1007/s10712-012-9207-x](https://doi.org/10.1007/s10712-012-9207-x)
- Dee DP et al (2011) The ERA-Interim reanalysis: configuration and performance of the data assimilation system. *Q J R Meteorol Soc* 137:553–597. doi:[10.1002/qj.828](https://doi.org/10.1002/qj.828)
- Draper CS, Reichle RH, De Lannoy GJM, Liu Q (2012) Assimilation of passive and active microwave soil moisture retrievals. *Geophys Res Lett* 39:L04401. doi:[10.1029/2011GL050655](https://doi.org/10.1029/2011GL050655)
- Drusch M (2007) Initializing numerical weather prediction models with satellite derived surface soil moisture: data assimilation experiments with ECMWF's Integrated Forecast System and the TMI soil moisture data set. *J Geophys Res* 112:D03102. doi:[10.1029/2006JD007478](https://doi.org/10.1029/2006JD007478)
- Drusch M, Wood EF, Gao H (2005) Observation operators for the direct assimilation of TRMM microwave imager retrieved soil moisture. *Geophys Res Lett* 32:L15403. doi:[10.1029/2005GL023623](https://doi.org/10.1029/2005GL023623)
- Ducharne A, Koster RD, Suarez MJ, Stieglitz M, Kumar P (2000) A catchment-based approach to modeling land surface processes in a general circulation model, 2: parameter estimation and model demonstration. *J Geophys Res* 105(20):24823–24838
- Dunne S, Entekhabi D (2006) Land surface state and flux estimation using the ensemble Kalman smoother during the Southern Great Plains 1997 field experiment. *Water Resour Res* 42:W01407. doi:[10.1029/2005WR004334](https://doi.org/10.1029/2005WR004334)
- Durand M, Margulis S (2008) Effects of uncertainty magnitude and accuracy on assimilation of multi-scale measurements for snowpack characterization. *J Geophys Res* 113:D02105. doi:[10.1029/2007JD008662](https://doi.org/10.1029/2007JD008662)
- Durand M, Andreadis KM, Alsdorf DE, Lettenmaier DP, Moller D, Wilson MD (2008) Estimation of bathymetric depth and slope from data assimilation of swath altimetry into a hydrodynamic model. *Geophys Res Lett* 35:L20401. doi:[10.1029/2008GL034150](https://doi.org/10.1029/2008GL034150)

- Durand M, Fu LL, Lettenmaier DP, Alsdorf D, Rodríguez E, Esteban-Fernandez D (2010) The Surface Water and Ocean Topography mission: observing terrestrial surface water and oceanic submesoscale eddies. *Proc IEEE* 98:766–779
- Ek M, Mitchell K, Yin L, Rogers P, Grunmann P, Koren V, Gayno G, Tarpley JD (2003) Implementation of Noah land surface model advances in the NCEP operational mesoscale Eta model. *J Geophys Res* 108(D22):8851. doi:[10.1029/2002JD003296](https://doi.org/10.1029/2002JD003296)
- Entekhabi D et al (2010) The Soil Moisture Active and Passive (SMAP) mission. *Proc IEEE* 98:704–716. doi:[10.1109/JPROC.2010.2043918](https://doi.org/10.1109/JPROC.2010.2043918)
- Evensen G (2003) The ensemble Kalman filter: theoretical formulation and practical implementation. *Ocean Dyn* 53:343–367. doi:[10.1007/s10236-003-0036-9](https://doi.org/10.1007/s10236-003-0036-9)
- Eyre JR, Kelly GA, McNally AP, Andersson E, Persson A (1993) Assimilation of TOVS radiance information through one-dimensional variational analysis. *Q J R Meteorol Soc* 119:1427–1463. doi:[10.1002/qj.49711951411](https://doi.org/10.1002/qj.49711951411)
- Forman BA, Reichle RH, Rodell M (2012) Assimilation of terrestrial water storage from GRACE in a snow-dominated basin. *Water Resour Res* 48:W01507. doi:[10.1029/2011WR011239](https://doi.org/10.1029/2011WR011239)
- Forman BA, Reichle RH, Derksen C (2013) Estimating passive microwave brightness temperature over snow-covered land in North America using a land surface model and an artificial neural network. *IEEE Trans Geosci Remote Sens* (in press)
- Foster JL, Sun C, Walker JP, Kelly R, Chang A, Dong J, Powell H (2005) Quantifying the uncertainty in passive microwave snow water equivalent observations. *Remote Sens Environ* 92(2):187–203
- Foster JL et al (2011) A blended global snow product using visible, passive microwave and scatterometer satellite data. *Int J Remote Sens* 32(5):1371–1395. doi:[10.1080/01431160903548013](https://doi.org/10.1080/01431160903548013)
- Gao Y, Xie H, Lu N, Yao T, Liang T (2010) Toward advanced daily cloud-free snow cover and snow water equivalent products from Terra-Aqua MODIS and Aqua AMSR-E measurements. *J Hydrol* 385:23–35
- Hall DK, Riggs GA (2007) Accuracy assessment of the MODIS snow products. *Hydrol Process* 21:1534–1547
- Hall DK, Riggs GA, Foster JL, Kumar SV (2010) Development and evaluation of a cloud-gap-filled MODIS daily snow-cover product. *Remote Sens Environ* 114:496–503
- Hilker T, Hall FG, Tucker CJ, Coops NC, Black TA, Nichol CJ, Sellers PJ, Barr A, Hollinger DY, Munger JW (2012) Data assimilation of photosynthetic light-use efficiency using multi-angular satellite data: II. Model implementation and validation. *Remote Sens Environ* 121:287–300
- Horwath M, Lemoine J-M, Biancale R, Bourgoigne S (2011) Improved GRACE science results after adjustment of geometric biases in the Level-1B K-band ranging data. *J Geod* 85(1):23–38
- Houborg R, Rodell M, Li B, Reichle RH, Zaitchik BF (2012) Drought indicators based on model assimilated GRACE terrestrial water storage observations. *Water Resour Res* 48:W07525. doi:[10.1029/2011WR011291](https://doi.org/10.1029/2011WR011291)
- Jackson TJ et al (2010) Validation of Advanced Microwave Scanning Radiometer soil moisture products. *IEEE Trans Geosci Remote Sens* 48:4256–4272. doi:[10.1109/TGRS.2010.2051035](https://doi.org/10.1109/TGRS.2010.2051035)
- Joiner J, Dee DP (2000) An error analysis of radiance and suboptimal retrieval assimilation. *Q J R Meteorol Soc* 126:1495–1514. doi:[10.1002/qj.49712656514](https://doi.org/10.1002/qj.49712656514)
- Kaminski T, Knorr W, Scholze M, Gobron N, Pinty B, Giering R, Mathieu P-P (2012) Consistent assimilation of MERIS FAPAR and atmospheric CO₂ into a terrestrial vegetation model and interactive mission benefit analysis. *Biogeosciences* 9:3173–3184. doi:[10.5194/bg-9-3173-2012](https://doi.org/10.5194/bg-9-3173-2012)
- Kelly RE (2009) The AMSR-E snow depth algorithm: description and initial results. *J Remote Sens Soc Jpn* 29:307–317
- Kerr Y et al (2010) The SMOS mission: new tool for monitoring key elements of the global water cycle. *Proc IEEE* 98(5):666–687
- Kim Y, Kimball JS, McDonald KC, Glassy J (2010) Developing a global data record of daily landscape freeze/thaw status using satellite passive microwave remote sensing. *IEEE Trans Geosci Remote Sens* 49:949–960. doi:[10.1109/TGRS.2010.2070515](https://doi.org/10.1109/TGRS.2010.2070515)
- Knorr W, Kaminski T, Scholze M, Gobron N, Pinty B, Giering R, Mathieu P-P (2010) Carbon cycle data assimilation with a generic phenology model. *J Geophys Res* 115:G04017. doi:[10.1029/2009JG001119](https://doi.org/10.1029/2009JG001119)
- Knowles KW, Savoie MH, Armstrong RL, Brodzik MJ (2006) Updated 2012. AMSR-E/Aqua daily EASE-grid brightness temperatures, September 2002 through May 2011. National Snow and Ice Data Center, Boulder, Colorado USA. Digital media
- Koster RD, Suarez MJ, Ducharme A, Stieglitz M, Kumar P (2000) A catchment-based approach to modeling land surface processes in a general circulation model, 1: model structure. *J Geophys Res* 105(20):24809–24822

- Kumar SV, Reichle RH, Peters-Lidard CD, Koster RD, Zhan X, Crow WT, Eylander JB, Houser PR (2008a) A land surface data assimilation framework using the Land Information System: description and applications. *Adv Water Resour* 31:1419–1432. doi:[10.1016/j.advwatres.2008.01.013](https://doi.org/10.1016/j.advwatres.2008.01.013)
- Kumar SV, Peters-Lidard C, Tian Y, Reichle R, Geiger J, Alonge C, Eylander J, Houser P (2008b) An integrated hydrologic modeling and data assimilation framework. *IEEE Comput* 41:52–59. doi:[10.1109/MC.2008.511](https://doi.org/10.1109/MC.2008.511)
- Kumar SV, Reichle RH, Harrison KW, Peters-Lidard CD, Yatheendradas S, Santanello JA (2012) A comparison of methods for a priori bias correction in soil moisture data assimilation. *Water Resour Res* 48:W03515. doi:[10.1029/2010WR010261](https://doi.org/10.1029/2010WR010261)
- Lahoz W, De Lannoy GJM (2013) Closing the gaps in our knowledge of the hydrological cycle over land: conceptual problems. *Surv Geophys*. doi:[10.1007/s10712-013-9221-7](https://doi.org/10.1007/s10712-013-9221-7)
- Li L, Gaiser P, Jackson T, Bindlish R, Du J (2007) WindSat soil moisture algorithm and validation. In: *IEEE international geoscience and remote sensing symposium* 23–28 July 2007, pp 1188–1191. doi:[10.1109/IGARSS.2007.4423017](https://doi.org/10.1109/IGARSS.2007.4423017)
- Li B, Rodell M, Zaitchik BF, Reichle RH, Koster RD, van Dam TM (2012) Assimilation of GRACE terrestrial water storage into a land surface model: evaluation and potential value for drought monitoring in western and central Europe. *J Hydrol* 446–447:103–115. doi:[10.1016/j.jhydrol.2012.04.035](https://doi.org/10.1016/j.jhydrol.2012.04.035)
- Liu Q, Reichle RH, Bindlish R, Cosh MH, Crow WT, de Jeu R, De Lannoy GJM, Huffman GJ, Jackson TJ (2011a) The contributions of precipitation and soil moisture observations to the skill of soil moisture estimates in a land data assimilation system. *J Hydrometeorol* 12:750–765. doi:[10.1175/JHM-D-10-05000.1](https://doi.org/10.1175/JHM-D-10-05000.1)
- Liu YY, Parinussa RM, Dorigo WA, de Jeu RAM, Wagner W, van Dijk AIJM, McCabe MF, Evans JP (2011b) Developing an improved soil moisture dataset by blending passive and active microwave satellite-based retrievals. *Hydrol Earth Syst Sci* 15(2):425–436. doi:[10.5194/hess-15-425-2011](https://doi.org/10.5194/hess-15-425-2011)
- Margulis SA, McLaughlin D, Entekhabi D, Dunne S (2002) Land data assimilation and estimation of soil moisture using measurements from the Southern Great Plains 1997 field experiment. *Water Resour Res* 38:1299. doi:[10.1029/2001WR001114](https://doi.org/10.1029/2001WR001114)
- Muñoz Sabater J, Rüdiger C, Calvet J-C, Fritz N, Jarlan L, Kerr Y (2008) Joint assimilation of surface soil moisture and LAI observations into a land surface model. *Agric For Meteorol* 148:1362–1373
- Njoku EG, Jackson TJ, Lakshmi V, Chan TK, Nghiem SV (2003) Soil moisture retrieval from AMSR-E. *IEEE Trans Geosci Remote Sens* 41:215–229. doi:[10.1109/TGRS.2002.808243](https://doi.org/10.1109/TGRS.2002.808243)
- Pan M, Wood EF (2006) Data assimilation for estimating the terrestrial water budget using a constrained ensemble Kalman filter. *J Hydrometeorol* 7:534–547
- Pan M, Wood EF, Wojcik R, McCabe MF (2008) Estimation of regional terrestrial water cycle using multi-sensor remote sensing observations and data assimilation. *Remote Sens Environ* 112:1282–1294. doi:[10.1016/j.rse.2007.02.039](https://doi.org/10.1016/j.rse.2007.02.039)
- Parinussa RM, Holmes TRH, de Jeu RAM (2012) Soil moisture retrievals from the WindSat spaceborne polarimetric microwave radiometer. *IEEE Trans Geosci Remote Sens*. doi:[10.1109/TGRS.2011.2174643](https://doi.org/10.1109/TGRS.2011.2174643)
- Pulliainen J (2006) Mapping of snow water equivalent and snow depth in boreal and subarctic zones by assimilating space-borne microwave radiometer data and ground-based observations. *Remote Sens Environ* 101:257–269
- Reichle RH (2012) The MERRA-land data product (Version 1.1). NASA Global Modeling and Assimilation Office, Office Note No. 3. Available at <http://gmao.gsfc.nasa.gov/pubs/>
- Reichle RH, Koster RD (2003) Assessing the impact of horizontal error correlations in background fields on soil moisture estimation. *J Hydrometeorol* 4:1229–1242
- Reichle RH, Koster RD (2004) Bias reduction in short records of satellite soil moisture. *Geophys Res Lett* 31:L19501. doi:[10.1029/2004GL020938](https://doi.org/10.1029/2004GL020938)
- Reichle RH, Koster RD (2005) Global assimilation of satellite surface soil moisture retrievals into the NASA catchment land surface model. *Geophys Res Lett* 32:L02404. doi:[10.1029/2004GL021700](https://doi.org/10.1029/2004GL021700)
- Reichle RH, Entekhabi D, McLaughlin DB (2001) Downscaling of radiobrightness measurements for soil moisture estimation: a four-dimensional variational data assimilation approach. *Water Resour Res* 37:2353–2364. doi:[10.1029/2001WR000475](https://doi.org/10.1029/2001WR000475)
- Reichle RH, McLaughlin DB, Entekhabi D (2002a) Hydrologic data assimilation with the ensemble Kalman filter. *Mon Weather Rev* 130:103–114
- Reichle RH, Walker JP, Koster RD, Houser PR (2002b) Extended vs. ensemble Kalman filtering for land data assimilation. *J Hydrometeorol* 3:728–740
- Reichle RH, Koster RD, Liu P, Mahanama SPP, Njoku EG, Owe M (2007) Comparison and assimilation of global soil moisture retrievals from the Advanced Microwave Scanning Radiometer for the Earth

- Observing System (AMSR-E) and the Scanning Multichannel Microwave Radiometer (SMMR). *J Geophys Res* 112:D09108. doi:[10.1029/2006JD008033](https://doi.org/10.1029/2006JD008033)
- Reichle RH, Crow WT, Koster RD, Sharif H, Mahanama SPP (2008a) Contribution of soil moisture retrievals to land data assimilation products. *Geophys Res Lett* 35:L01404. doi:[10.1029/2007GL031986](https://doi.org/10.1029/2007GL031986)
- Reichle RH, Crow WT, Keppenne CL (2008b) An adaptive ensemble Kalman filter for soil moisture data assimilation. *Water Resour Res* 44:W03423. doi:[10.1029/2007WR006357](https://doi.org/10.1029/2007WR006357)
- Reichle RH, Bosilovich MG, Crow WT, Koster RD, Kumar SV, Mahanama SPP, Zaitchik BF (2009) Recent advances in land data assimilation at the NASA global modeling and assimilation office. In: Park SK, Xu L (eds) *Data assimilation for atmospheric, oceanic and hydrologic applications*. Springer, New York, pp 407–428. doi:[10.1007/978-3-540-71056-1](https://doi.org/10.1007/978-3-540-71056-1)
- Reichle RH, Koster RD, De Lannoy GJM, Forman BA, Liu Q, Mahanama SPP, Toure A (2011) Assessment and enhancement of MERRA land surface hydrology estimates. *J Clim* 24:6322–6338. doi:[10.1175/JCLI-D-10-05033.1](https://doi.org/10.1175/JCLI-D-10-05033.1)
- Rienecker MM et al (2008) The GEOS-5 data assimilation system—documentation of versions 5.0.1 and 5.1.0, and 5.2.0. NASA Tech. Rep. Series on Global Modeling and Data Assimilation, NASA/TM-2008-104606, vol 27, 92 pp. Available at <http://gmao.gsfc.nasa.gov/pubs/>
- Rienecker MM et al (2011) MERRA—NASA's Modern-Era Retrospective analysis for Research and Applications. *J Clim* 24:3624–3648. doi:[10.1175/JCLI-D-11-00015.1](https://doi.org/10.1175/JCLI-D-11-00015.1)
- Rodell M et al (2003) The global land data assimilation system. *Bull Am Meteorol Soc* 85:381–394. doi:[10.1175/BAMS-85-3-381](https://doi.org/10.1175/BAMS-85-3-381)
- Rodell M, Velicogna I, Famiglietti JS (2009) Satellite-based estimates of groundwater depletion in India. *Nature* 460:999–1002. doi:[10.1038/nature08238](https://doi.org/10.1038/nature08238)
- Rowlands DD, Luthcke SB, Klosko SM, Lemoine FGR, Chinn DS, McCarthy JJ, Cox CM, Anderson OB (2005) Resolving mass flux at high spatial and temporal resolution using GRACE intersatellite measurements. *Geophys Res Lett* 32:L04310. doi:[10.1029/2004GL021908](https://doi.org/10.1029/2004GL021908)
- Rowlands DD, Luthcke SB, McCarthy JJ, Klosko SM, Chinn DS, Lemoine FG, Boy J-P, Sabaka TJ (2010) Global mass flux solutions from GRACE: a comparison of parameter estimation strategies—mass concentrations versus Stokes coefficients. *J Geophys Res* 115:B01403. doi:[10.1029/2009JB006546](https://doi.org/10.1029/2009JB006546)
- Sahoo AK, De Lannoy GJM, Reichle RH, Houser PR (2012) Assimilation and downscaling of satellite observed soil moisture over the little river experimental watershed in Georgia, USA. *Adv Water Resour* 52:19–33. doi:[10.1016/j.advwatres.2012.08.007](https://doi.org/10.1016/j.advwatres.2012.08.007)
- Schaefer GL, Cosh MH, Jackson TJ (2007) The USDA Natural Resources Conservation Service Soil Climate Analysis Network (SCAN). *J Atmos Ocean Technol* 24:2073–2077. doi:[10.1175/2007JTECH A930.1](https://doi.org/10.1175/2007JTECH A930.1)
- Seneviratne SI, Corti T, Davin EL, Hirschi M, Jaeger EB, Lehner I, Orlowsky B, Teuling AJ (2010) Investigating soil moisture–climate interactions in a changing climate: a review. *Earth Sci Rev* 99:125–161. doi:[10.1016/j.earscirev.2010.02.004](https://doi.org/10.1016/j.earscirev.2010.02.004)
- Smith AB et al (2012) The Murrumbidgee soil moisture monitoring network data set. *Water Resour Res* 48:W07701. doi:[10.1029/2012WR011976](https://doi.org/10.1029/2012WR011976)
- Stieglitz M, Ducharme A, Koster RD, Suarez M (2001) The impact of detailed snow physics on the simulation of snow cover and subsurface thermodynamics at continental scales. *J Hydrometeorol* 2: 228–242
- Stöckli R, Rutishauser T, Baker I, Liniger MA, Denning AS (2011) A global reanalysis of vegetation phenology. *J Geophys Res* 116:G03020. doi:[10.1029/2010JG001545](https://doi.org/10.1029/2010JG001545)
- Sturm M, Holmgren J, Liston GE (1995) A seasonal snow cover classification system for local to global applications. *J Clim* 8:1261–1283
- Sturm M, Taras B, Liston GE, Derksen C, Jonas T, Lea J (2010) Estimating snow water equivalent using snow depth data and climate classes. *J Hydrometeorol* 11:1380–1394
- Su H, Yang Z-L, Niu G-Y, Dickinson RE (2008) Enhancing the estimation of continental-scale snow water equivalent by assimilating MODIS snow cover with the ensemble Kalman filter. *J Geophys Res* 113:D08120. doi:[10.1029/2007JD009232](https://doi.org/10.1029/2007JD009232)
- Su H, Yang Z-L, Dickinson RE, Wilson CR, Niu G-Y (2010) Multisensor snow data assimilation at the continental scale: the value of gravity recovery and climate experiment terrestrial water storage information. *J Geophys Res* 115:D10104. doi:[10.1029/2009JD013035](https://doi.org/10.1029/2009JD013035)
- Swenson S, Wahr J (2006) Post-processing removal of correlated errors in GRACE data. *Geophys Res Lett* 33:L08402. doi:[10.1029/2005GL025285](https://doi.org/10.1029/2005GL025285)
- Tang Q, Gao H, Yeh P, Oki T, Su F, Lettenmaier DP (2010) Dynamics of terrestrial water storage change from satellite and surface observations and modeling. *J Hydrometeorol* 11:156–170
- Tedesco M, Narvekar PS (2010) Assessment of the NASA AMSR-E SWE product. *IEEE J Sel Top Appl Earth Obs Remote Sens* 3:141–159

- Tedesco M, Reichle R, Löw A, Markus T, Foster JL (2010) Dynamic approaches for snow depth retrieval from spaceborne microwave brightness temperature. *IEEE Trans Geosci Remote Sens* 48(4): 1955–1967
- Trenberth KE, Asrar G (2013) Challenges and opportunities in watercycle research: WCRP contributions. *Surv Geophys*. doi:[10.1007/s10712-012-9214-y](https://doi.org/10.1007/s10712-012-9214-y)
- Wagner W, Lemoine G, Rott H (1999) A method for estimating soil moisture from ERS scatterometer and soil data. *Remote Sens Environ* 70:191–207. doi:[10.1016/S0034-4257\(99\)00036-X](https://doi.org/10.1016/S0034-4257(99)00036-X)
- Wahr J, Swenson S, Zlotnicki V, Velicogna I (2004) Time-variable gravity from GRACE: first results. *Geophys Res Lett* 31:L11501. doi:[10.1029/2004GL019779](https://doi.org/10.1029/2004GL019779)
- Wigneron J-P et al (2007) L-band microwave emission of the biosphere (L-MEB) model: description and calibration against experimental data sets over crop fields. *Remote Sens Environ* 107:639–655
- Zaitchik BF, Rodell M, Reichle RH (2008) Assimilation of GRACE terrestrial water storage data into a land surface model: results for the Mississippi River basin. *J Hydrometeorol* 9:535–548. doi:[10.1175/2007JHM951.1](https://doi.org/10.1175/2007JHM951.1)
- Zhou Y, McLaughlin D, Entekhabi D (2006) Assessing the performance of the ensemble Kalman filter for land surface data assimilation. *Mon Weather Rev* 134:2128–2142